Answer to review #2

Thank you for your review. Here are the answers to your comments

This manuscript describes air quality simulations with EPA's CMAQ model over the contiguous United States with a focus on the use of dynamic chemical lateral boundary conditions from a global model, Geos-chem snd investigates the predictive skill for ozone and PM.5 with an emphasis on dust events and fires. CMAQ model predictions for air quality are improved with use of dynamic chemical lateral boundary conditions. The authors identify an important and timely problem and investigate it well. I recommend the paper for publication after the following items are addressed. There has been a lot of work on developing boundary conditions for CMAQ in particular and for aerosols in particular. That literature is not cited here and that surprises me. Can the authors put their work here In that context? Here is one example: https://gmd.copernicus.org/articles/7/339/2014/

- You are right that we missed some references. We added the reference that you referred and some corresponding statement in the introduction session.

This work may have implications for policy-relevant background and exceptional event determination. Can the authors provide any context for this?

- *This work is actually for supporting our operational forecast. We added some related statements in the introduction*

When discussing figure 10 in the manuscript the authors point out that they were unable to capture fireworks however the observed [PM2.5] peaks in figure 10 occur on July 5 not July 4. I understand the time is in UTC, but it looks to be a whole day apart and not just eight or nine hours.

- You are right that the local effect of firework emissions won't last long. However, most firework emission were injected in elevated levels, and the associated pollutants can be transported to extended downstream areas. If the downstream area are big and adjacent one another, the regional averaged effect could appear for a longer time. The following figure show the observed PM2.5 over single state (Oregon) and EPA region 8 (three states), and the effect of fireworks obviously last longer in the area of three states than that in one state, as the EPA region 10 represents a bigger receptor area. In Figure 10, the Northcentral region includes 9 states, and Northeastern region represents 12 states, which are much bigger than the EPA region 10. So it is not surprised that the effect could last so long since the receptor areas are so big that the transported pollutants have enough time

to affect extended downstream areas before moving out of the region.

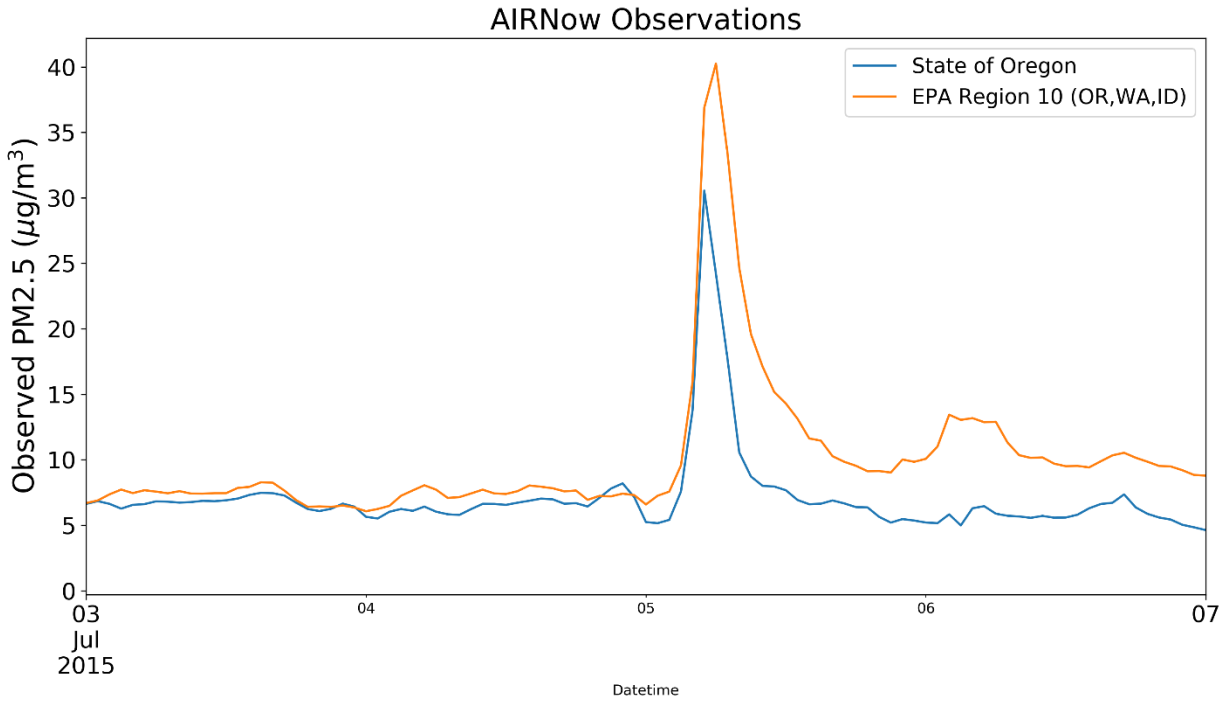

Sonntag et al., 2014 is not the best reference for AERO6.

- You are right. We added another one (Foley, 2010, https://doi.org/10.5194/gmd-3-205-2010)

Please provide a link or reference for the wild fire emission method?

- Added a reference https://doi.org/10.5194/gmd-13-2169-2020

Thank you again for your comments

Answer to review #1

Thank you for your review. We made comprehensive revisions according to your suggestion. The figures 13/14 were re-plotted and added another run for summer 2018 case. Here are the answers to your comments

Review of Tang et al. "Comparison of Chemical Lateral Boundary Conditions for Air Quality Predictions over the Contiguous United States during Intrusion Events" In this paper, Tang et al., use a number of different methods to set boundary conditions for use in CMAQ as part of the US NOAAs forecasting system. While focusing on PM2.5, they also looked at ozone. Not surprisingly, they found that having boundary conditions that are more representative of actual conditions improved model performance. The manuscript needs to be thoroughly edited for grammar before resubmission. It is replete with incorrect inclusion or exclusion of articles (in the grammatical sense).

- Thank you for your comments. We follow your suggestions to make the literature revision and correct the gramma issues. Please see below for the details.

They also inconsistently used plurals and singulars, including when the used the terms LBC(s) and CLBC(s). Given that you typically set more than one boundary condition, it should almost always be plural, but either way, be consistent. They tend to use ambiguous ronouns (e.g., its).

- Great suggestion. We made changes to be consistent. The LBC(s) and CLBC(s) are used in three circumstances: general term, one LBC vs another LBC, and several LBCs. Now the plural word is used under only the third circumstance.

After fighting through the manuscript, the third sentence of the Conclusion was: "The GEOS dynamic LBC showed the overall best score when comparing with the surface observations during the June-July 2015 while Saharan dust intrusion and Canadian wildfire events occurred." "LBC" should be "LBCs", "comparing"should be "compared", "the June" should be "June", "while" should be "when", "Saharan" should be "the Saharan" (at least I think those are appropriate).

- Changed

In the Introduction, they state that there are two roles "it" (actually they, i.e., CLBCs) play. The two are the same. They are setting values of the concentrations used in solving the differential equations that underlie the core of an air quality model. In such a way, they might be called constraints, but that is both awkward and imprecise, as they are not setting a range, but an actual value. This is exactly how external influences are brought in to the model. Using the precise definition of boundary condition leads to (1) and (2) being the same.

- You are right that the CLBC has one value, though it can be static or dynamic. Now the sentence is changed to be "The CLBC sets concentration values along the regional domain's lateral boundary, and those setting values have two effects in the regional modeling system depending on the CLBC types (static or dynamic) and the events."

Line 14: "Proper" is not the best word here. What defines proper? Do they mean accurate? How accurate?

- You are right that a suitable word is needed here, and "proper" is not the best. We changed it to "certain" since regional model need a lateral boundary condition to run, regardless good or bad LBC.

Line 26: Sentence beginning Tang et al.: What point is being made?

- Changed. We added "For non-intrusion events,"

The description of the 5 model runs should be more clear, with specifics in a Table.

- Changed Table 1 to be clearer.

ACP is an international journal, so the US NOAA should be used at least the first time and NOAA defined.

- Added the definition of NOAA

Page 3 Line 34: : : Not sure what this is adding.

- Changed to "We developed a tool to extract the GEOS-LBC along the NAQFC's domain boundaries"

The title should be a bit more explanatory as Intrusions can be stratospheric, still impacting lateral boundary conditions.

- Changed to "pollutant intrusion events". Actually, the two GEOS-LBCs included stratospheric ozone influence (Figure S1) from the GEOS global model, which is the reason of their better correlations (Table 5). This study focused on influence on surface O3/PM2.5, so the stratospheric intrusion was not strongly highlighted.

Page 10, line 35. The surface stations reflect the wildfire intrusions just as well as VIIRs at their location. The issue here is how well the surface stations provide more spatial coverage.

- Yes, your words are better for what it actually means. We changed. In fact, we first tried to use surface monitoring data as indicators as that in-situ surface data is more reliable and has better temporal resolution (hourly). However, its poor spatial coverage is not good enough for this purpose.

Page 11, line 20: I do not think that "a high pressure system controlled western Canada" (the authors should look at that whole sentence).

- Changed to be Figure S4 showed that there was a high-pressure system with peak surface pressure up to 1022 hPa in the western Canada.

P3 L20-21. Why does the CMAQ_BASE simulation use a clean background for aerosols.

- We added the explanation. The clean background aerosol LBC was used in the operational NAQFC before the NGAC model data was available, since the CONUS domain's boundaries lay on the ocean or less polluted regions. Switched Figures 1 and 2.

According to the introduction, the NAQFC system currently uses NGAC for its aerosol LBCs? Does this not make the performance of the CMAQ_BASE simulation artificially worse than the current NAQFC system? And if your goal is to compare how new CLBCs impact the forecast, shouldn't the CMAQ_BASE simulation represent what is used in the current NAQFC system? It is not clear to me if any of the 5 simulations listed in Table 1 use the same CLBCs as the current NAQFC system, though I think it may be NGAC-LBC. This should be clarified.

- It was clarified in the introduction "The current NAQFC uses the dust-only aerosol CLBC from NGAC". So, current NAQFC just use the dust LBC from NGAC, not the full-GOCART aerosol LBC, as there were some issues in NGAC's other aerosol

prediction, including wildfire. The CMAQ_Base was not artificially worse, and that LBC was actually used in the old NAQFC system before NGAC was available.

Figure 7. There appears to be a discontinuity at the transition between the east and north boundaries. Is this correct, and if so, what could cause this?

- It is correct. CMAQ's boundary index is always from south to north and from west to east. So the boundary index's start points are reset instead of continuous for north and west boundaries. You can find the boundary structure in https://www.cmascenter.org/ioapi/documentation/all_versions/html/THKBDY.jpg. We added the explanation in Figure 3's captions.

If the details of the mapping are important, the chemical mapping is a bit haphazard. Putting all of the MVK in to ISPD would require that all of the MVK comes from isoprene. Splitting all of the INO2 using the coefficients in the ISOP+NO3 reaction would require that all of the species degrade at a similar rate, or that INO2 rapidly reacts to those products.

- Yes, you are right for these issues. GEOS model's MVK comes from Isoprene and there is no MVK emission. So the MVK mapping to ISPD of CMAQ's CB05 is consistent with its source in GEOS. For the intermediate INO2, GEOS has this explicit species, and it has the following reactions, such as INO2+MO2 → 0.55NO2 + 0.40HO2 + 0.425HNO3 + 0.025NO2 + 0.05MACR + 0.08CH2O + 0.03MVK + 0.25RCHO + 0.75CH2O + 0.25MOH + 0.25ROH + 0.05HO2. CMAQ's CB05 mechanism bypasses the intermediate INO2, and assumes ISOP+NO3 directly generate some similar final products. It is true that we can not achieve perfect consistence for these species mapping as these two mechanisms are so different. Fortunately, for the CONUS domain, the isoprene chemistry influence's on the CONUS LBC is less significant compared to the major intrusion events of wildfire plume and dust storm as the short-lived isoprene hardly reach farther downwind. I added the explanation.

ALK4 includes C4 and higher alkanes, so having it turned in to 4 PARs is biased low unless it is all butane isomers. A detailed understanding of both mechanisms are needed to do such a mapping directly if this step is important to be done in detail (which I am not sure it is: : : for boundary conditions, the important species are probably NO, NO2, O3, PM species, SO2, NH3, HCHO and a few others, but that is just a guess: they might check that out. Having to deal with large fires may lead to large fluxes of other organics that then become important. They need to work on a better way of expressing their finding that setting better boundary conditions leads to a better simulation.

- Yes, it is true that this treatment could have a "truncation error". However, the GEOS global model itself also treat the ALK4 mainly as butane: ALK4+OH → R4O2, R4O2+NO → NO2 + 0.32ACET + 0.19MEK + 0.18MO2 + 0.27HO2 + 0.32ALD2 + 0.13RCHO + 0.50A3O2 + 0.18B3O2 + 0.32ETO2, or Cn with n~4. For the LBC, the issue of C5 or higher alkanes treatment may only appear if strong C5+ alkane emissions existed outside of our domain and were not too far (penpane's lifetime is around 4.6 days (Helmig et al, 2014 (doi:10.5194/acp-14-1463-2014), and hexane has even short lifetime than butane), and the global model treated the C5+ alkanes emission and reaction more explicitly. For our cases, only big wildfire emission could have this impact in real world, though the wildfire C5+ alkane emission is at least one order of magnitude lower than the corresponding CO/Ethane/Propane emission (Urbanski et al, 2008, DOI:10.1016/S1474-8177(08)00004-1). Also the GEOS did not treat C5+ alkanes explicitly to capture the real-world situation. So, the C5+ alkane mapping for LBC unlikely make big difference

in our simulations with that "truncation error". In fact, the difference between GEOS and CMAQ's carbon bond mechanisms, and the uncertainty of wildfire emissions could be bigger issues, but they are beyond the content of this manuscript. We added some related explanations in the manuscript.

The results from the AOT-derived LBC to be a more compelling idea and would have liked to see a comparison of CMAQ performance using the AOT-derived LBC and the dynamic LBC (GEOS-LBC and NGAL-LBC), but these were not modeled for the same time period as the AOT-NLBC case. Is the use of three or four significant figures justified?

- Good suggestion. We added the NGAC-LBC for the summer 2018 comparison. Some related discussion and figures are also expanded.

In the end, there are aspects of this paper of potential interest to ACP readers, but at this juncture, the grammar and some of the set up needs work before it should be further considered for publication in ACPD or elsewhere. The authors need to identify and highlight what is unique about their findings other than "better boundary conditions lead to better results." What is the best approach and why? (or, what are the positives and negatives of each approach and what is a general recommendation after weighing those attributes?) This should be stated concisely in the Abstract and the conclusions, backed up with specific study results.

- Thank you for your encouragement. We revised the conclusions and abstract, and made thorough literature editing through the manuscript. Please see revised manuscript for detail.

Again. Thank you for your comments

Comparison of Chemical Lateral Boundary Conditions for Air Quality Predictions over the Contiguous United States during Pollutant Intrusion Events

Youhua Tang[1,2], Huisheng Bian[3,4], Zhining Tao[3,5], Luke D. Oman[3], Daniel Tong[1,2,6], Pius Lee[1], Patrick C. Campbell[1,2], Barry Baker[1,2], Cheng-Hsuan Lu[7,10], Li Pan[8,9], Jun Wang[8], Jeffery McQueen[8], Ivanka Stajner[8]

1. NOAA Air Resources Laboratory, College Park, MD 20740, USA
2. Center for Spatial Information Science and Systems, George Mason University, Fairfax, VA
3. NASA Goddard Space Flight Center, Greenbelt, MD
4. University of Maryland at Baltimore County, Baltimore, MD
5. Universities Space Research Association, Columbia, MD 21046
6. University of Maryland, College Park, MD 20740, USA
7. Joint Center for Satellite Data Assimilation, Boulder, CO, USA
8. NOAA/NCEP/Environmental Modeling Center, College Park, MD, USA
9. I.M. Systems Group Inc., Rockville, MD
10. University at Albany, State University of New York, Albany, NY, USA

Abstract

The existing National Air Quality Forecast Capability (NAQFC) operated at NOAA provides operational forecast guidance for ozone and particle matters with aerodynamic diameter less than 2.5µm ($PM_{2.5}$) over the contiguous 48 U.S. states (CONUS) using the Community Multi-scale Air Quality (CMAQ) model. The existing NAQFC uses a climatological chemical lateral boundary condition (CLBC), which cannot capture pollutant intrusion events originated outside of the model domain. In this study, we developed a model framework to use a dynamic CLBC from the Goddard Earth Observing System Model, version 5 (GEOS) to drive NAQFC. The method of mapping GEOS chemical species to CMAQ CB05-Aero6 species was developed. We evaluated NAQFC's performance using the new CLBC from GEOS. The utilization of the GEOS dynamic CLBC showed an overall best score when comparing the NAQFC simulation with the surface observations during the Saharan dust intrusion and Canadian wildfire events in summer 2015: the PM2.5 correlation coefficient R was improved from 0.18 to 0.37 and the mean bias was narrowed from -6.74 µg/m^3 to -2.96 µg/m^3 over CONUS. The influences of CLBCs depend not only on the distance from the inflow boundary, but also on the related species and their regional characteristics. For the PM2.5 prediction, the CLBC's effect on the model's correlations was mainly near the inflow boundary, and its impact on the background concentrations could reach farther inside the domain. The CLBCs could affect background ozone through the inflows of ozone itself and its precursors. It was further found that aerosol optical thickness (AOT) from VIIRS retrieval correlated well to the column CO and elemental carbon from GEOS. Based on this correlation, we tested deriving the new CLBC for wildfire intrusion events. The AOT derived CLBC showed good skills for the wildfire intrusion events for summer 2018 as a case study. It can be a useful alternative in case a reliable CLBC of GEOS is not available.

Deleted: the
Deleted: Currently
Deleted: is using
Deleted: s
Deleted: C
Deleted: s
Deleted: from a monthly climatology
Deleted: introduce
Deleted: the
Deleted: time-varying
Deleted: chemical
Deleted: simulation
Deleted: as the CLBCs
Deleted: also
Deleted: then
Deleted: C
Deleted: s
Deleted: C
Deleted: s
Deleted: CLBCs'
Deleted: ed
Deleted: not only
Deleted: C
Deleted: also
Deleted: altered
Deleted: ,
Deleted: based
Deleted: which
Deleted: s
Deleted: was derived
Deleted: s
Deleted: successfully captured
Deleted: in our case study
Deleted: the
Deleted: s
Deleted: are

1. Introduction

The chemical lateral boundary condition (CLBC) is one of the most important factors affecting the prediction accuracy of regional chemical transport models (Tang et al., 2009; Tang et al., 2007). The CLBC sets concentration values along the regional domain's lateral boundary, and those setting values have two effects in the regional modeling system depending on the CLBC types (static or dynamic) and the events. One effect is imposing a constraint with static background concentrations for some long-lived pollutants, such as CO and O_3, which is the typical role of the climatological CLBC for non-intrusion events. Models like the Community Air Quality Multi-scale Model (CMAQ) hemispheric version (Mathur et al, 2017) can also get this constraint with its CLBC along the equator. The second effect of the CLBC, representing the influences of external intrusion events, can only be achieved with dynamic (time-varying) CLBC. This CLBC can come from a global model, or a regional model with a bigger domain (Tang et al., 2007), or observed profiles (Tang et al., 2009). Henderson et al (2014) compiled a 10-year CLBCs database over the Contiguous United States (CONUS) using a global chemical transport model (GEOS-Chem, Bey et al., 2001) and evaluated it against satellite retrieved ozone and CO vertical profiles.

As a regional chemical forecast system, the existing National Air Quality Forecast Capability (NAQFC) operated in the National Oceanic and Atmospheric Administration (NOAA) of the United States needs certain CLBC for its daily prediction. The current NAQFC uses the dust-only aerosol CLBC from the NOAA Environmental Modeling System (NEMS) Global Forecast System (GFS) Aerosol Component (NGAC) (Lu et al, 2016; Wang et al, 2018), which is the GFS model coupled with Goddard Chemistry Aerosol Radiation and Transport (GOCART) aerosol mechanism (Chin et al., 2000, 2002; Colarco et al., 2010). Before the implementation of NGAC CLBC, NAQFC used a background static profile LBC for aerosols described in Lee et al. (2017). For gaseous species, NAQFC uses a modified monthly averaged LBC from the GEOS-Chem simulation for 2006 (Pan et al., 2014). To alleviate surface ozone over-predictions, the upper tropospheric ozone LBC from GEOS-Chem has been limited ≤ 100 ppbV.

The static CLBC cannot capture the signals of some intrusion events, such as the biomass burning plumes from the outside of the domain, which could affect ozone and particle matter with aerodynamic diameter less than 2.5μm ($PM_{2.5}$). For non-intrusion events, Tang et al. (2007) investigated the sensitivity of the regional chemical transport model (RCTM) to CLBCs, and found that the background magnitude of the pollutant concentrations sometimes were more important than the variation of the CLBC for the near-surface prediction over polluted areas, or the first effect of the CLBC was more critical. Over the CONUS domain, the prevailing inflow lateral boundary includes northern and western USA, where Canadian emission and long-range transported Asian air-masses can affect the CONUS background. Southeastern States could encounter the Saharan dust intrusion during summer time, which usually resulted in a surface PM2.5 increase (Lu et al, 2016). In order to assess their impact and support the operational

Deleted: is

Formatted: Font: (Default) Times New Roman, 12 pt

Deleted: It mainly

Deleted: plays

Deleted: roles

Deleted: : 1)

Deleted: to

Deleted: e

Deleted: the

Deleted: s

Deleted: and 2) to represent the external influence for intrusion events

Deleted: The climatological static CLBCs can provide the first role for some long-lived pollutants, such as CO and O_3.

Deleted: role

Deleted: made

Deleted: the

Deleted: s

Deleted: Such

Deleted: s

Deleted: only

Deleted: at

Deleted: proper

Deleted: s

Deleted: the

Deleted: the

Deleted: s

Deleted: (Bey et al., 2001)

Deleted: year

Deleted: have

Deleted: gaseous

Deleted:

Deleted: s

Deleted: role

Deleted: Contiguous United States (

Deleted:)

regional air quality forecast, we need a CLBC from global models with those signals. In this study, we extracted the CLBC from the GEOS global chemical circulation model (GCCM) (Strode et al. 2019; Molod et al., 2012) in static (monthly average) and dynamic (every 3 hours) modes. The CMAQ runs with the GEOS CLBC were then compared to the CMAQ base case and another run with the NGAC aerosol LBC for the summer 2015. During this period, the Canadian wildfire and Sahara dust affected the CONUS domain, which affected the Northern and Southern USA, respectively, and different CLBCs showed their impacts on the CMAQ regional predictions. In addition, we will investigate the method of using historical CLBCs with a certain indicator to derive a new CLBC for the future pollutant intrusion events in case an appropriate global CLBC is not available.

Deleted: a proper
Deleted: a
Deleted: that carries
Deleted: is needed
Deleted: -
Deleted: varying
Deleted: s
Deleted:

2. Model Configuration and Experiment Design

Current NAQFC is using CMAQ version 5.0.2, which includes CB05 gaseous chemical mechanism (Yarwood et al., 2005) with updated toluene (Whitten et al., 2010) and chlorine chemistry (Tanaka et al., 2003; Sarwar et al., 2007), and Aero6 (Foley et al., 2010; Sonntag et al., 2014) aerosol module driven by NOAA/NCEP's North American Mesoscale Model (NAM) forecasting. It has 12km horizontal resolution covering CONUS and 35 vertical layers up to 100 hPa. Anthropogenic and mobile emissions are the projected U.S. EPA National Emission Inventory (NEI) with base year 2011 and the point emissions have been updated with the U.S. EPA Continuous Emission Monitoring System (CEMS) for the target year (2015). Biogenic emissions are based on the Biogenic Emission Inventory System (BEIS) 3.14 (Pierce et al., 1998). Wildfire emission inside the CONUS domain is estimated using the U.S. Forest Service (USFS) BlueSky fire emissions estimation algorithm with the fire location information provided by NOAA Hazard Mapping System (HMS), which is a satellite-based fire detection system with some manual analysis. The detailed wildfire emission process of this system was described in Pan et al. (2020).

In this study, we conducted 5 model runs with different CLBCs (Table 1). The CMAQ base case (referred to as CMAQ_Base) uses the modified GEOS-CHEM 2006 monthly gaseous LBC and clean aerosol background, same as the LBC used in the earlier NAQFC system before the NGAC model data was available. The NAQFC CONUS domain covers southern Canada and Northern Mexico with three boundaries over sea water: western boundary over the Pacific Ocean, Eastern boundary over the Atlantic Ocean, and half Southern boundary over the Gulf of Mexico (Figure 1). Most of Canadian anthropogenic emissions are located in Southern Canada covered by the NAQFC domain. During the most non-intrusion periods, the inflow air masses over the boundaries were relatively less polluted. The NGAC-LBC contains NGAC's GOCART aerosol dynamic LBC. The GEOS dynamic LBC (GEOS-LBC) has full chemistry for both gaseous and aerosol species. We also tested its corresponding monthly mean LBC (GLBC-monthly) for the temporal variation. Besides the normal global LBCs, an aerosol optical depth (AOT) derived Northern LBC (AOT-NLBC) is developed, which will be discussed later. These runs used the

Deleted:
Deleted: (referred to as CMAQ_Base).
Deleted: is

same settings except their CLBCs. The two CMAQ runs with dynamic CLBCs, the NGAC-LBC and GEOS-LBC, are updated every 3 hours. The NGAC-LBC only updates the aerosol LBC from the NGAC global model and it uses the same static gaseous LBC as that of the CMAQ Base. The GEOS-LBC includes dynamic variation for both the gaseous and aerosol species. The GLBC-monthly is the static CLBC generated from the monthly mean GCCM results, or temporal averaged GEOS-LBC. The AOT-NLBC is the same as the GLBC-monthly except that its northern boundary condition is generated from the relationship of VIIRS (Visible Infrared Imaging Radiometer Suite) AOT and GEOS-LBC for the wildfire intrusion events, which will be described later.

We developed a tool to extract the GEOS-LBC along the NAQFC's domain boundaries. It is based on the existing Global-to-Regional interfaces developed by Tang et al (2008, 2007) for MOZART, RAQMS, and NGAC global models with the enhancement to support GEOS's NetCDF4 format, vertical layers and chemical species. This tool includes two major functions: spatial mapping and species mapping. Spatially, GEOS's concentrations from its 576×361 grid in the 0.625°×0.5° horizontal resolution with 72 vertical layers are 3-dimensionally interpolated into CMAQ's CONUS lateral boundary periphery in the 12 km horizontal resolution. Since the different chemical mechanisms have been employed in global chemical transport models and CMAQ, the species mapping is required to link both models.

2.1 Gaseous Species Mapping

The GCCM outputs 122 gaseous chemical species and 15 aerosol species. For the species such as O_3, CO, NO, and NO_2, an explicit one-on-one mapping can be achieved. However, some voltaic organic compounds (VOCs) need special treatment during the conversion as GEOS uses different lumping approaches from the CMAQ CB05tucl (carbon bond 5 mechanism with toluene and chloride species). Table 2 lists the VOC species map used to convert GCCM's gaseous species to CMAQ's CB05tucl species. Two methods were employed for VOCs' speciation mapping: one was based on the carbon bond structure, e.g. ALK4 → 4 PAR (Table 2), and the other was based on the similarity of the reactions. For instance, in the GEOS, the products of isoprene reaction with NO3 are lumped into INO2, an intermediate RO2 radical.

ISOP + NO3 → INO2

The radical INO2 participates in the following reactions (Eastham et al., 2014;Tyndall et al., 2001)

INO2 + NO → 1.10NO2 + 0.80HO2 +0.85HNO3 + 0.05NO2 + 0.10MACR + 0.15CH2O + 0.05MVK

INO2 + HO2 → INPN

INO2 + MO2 → 0.55NO2 + 0.40HO2 + 0.425HNO3 + 0.025NO2 + 0.05MACR + 0.08CH2O + 0.03MVK + 0.25RCHO + 0.75CH2O + 0.25MOH + 0.25ROH + 0.05HO2

Deleted: imported the corresponding LBC
Deleted: every
Deleted:
Deleted: s
Deleted: its
Deleted: are the same as th
Deleted: e CMAQ
Deleted: base
Deleted: case
Deleted: provides
Deleted: LBCs
Deleted: LBC
Deleted: GEOS
Deleted: An interface between NAQFC and GEOS has been developed to transfer CLBC
Deleted: s
Deleted: e interface
Deleted:
Deleted: are
Deleted:
Deleted: GCCM
Formatted: Left
Formatted: Font: (Default) Times New Roman
Formatted: Left, Space After: 0 pt, Line spacing: single, Don't adjust space between Latin and Asian text, Don't adjust space between Asian text and numbers
Formatted: Font: (Default) Times New Roman
Formatted: Font: (Default) Times New Roman
Formatted: Font: (Default) Times New Roman

INO2 + MCO3 → MO2 + 0.10NO2 + 0.80HO2 + 0.85HNO3 + 0.05NO2 + 0.10MACR + 0.15CH2O + 0.05MVK

INO2+MCO3 → RCHO + ACTA + NO2

The CB05tucl mechanism skips the intermediate INO2, and directly represents it as

ISOP + NO3 = 0.200*ISPD + 0.800*NTR + XO2 + 0.800*HO2 + 0.200*NO2 + 0.800*ALDX + 2.400*PAR

Therefore, the GEOS species of INO2 is split into seven CB05tucl species with the corresponding factors, respectively (Table 2). It should be noted that this conversion is just an approximation, and we can not achieve perfect consistency for these species mapping as these two mechanisms are so different, especially for the complex isoprene chemistry. Fortunately, for the CONUS domain, the isoprene chemistry influence on the CONUS LBC is less significant compared to the major intrusion events of wildfire plume and dust storm. Most biogenic emitted species are short-lived, and their direct impact on LBC is relatively weak, as they could not be transported farther downstream. A similar situation can also be applied to other short-lived species, such as NOx, which will be discussed later. However, these biogenic emissions can affect local photochemical processes, and generate relatively long-lived species, such as ozone and NTR, outside of our regional domain, which have more chance to reach the LBC and affect downstream. Fortunately, most of these secondary long-lived species are explicitly included in these two mechanisms, and can be directly mapped.

Some species are represented explicitly in the GEOS, such as methyl vinyl ketone (MVK), which is lumped in CB05tucl's isoprene product (ISPD). In GEOS, the MVK mainly comes from the Isoprene, which is consistent with the CMAQ's ISPD source. Some GEOS species can also be mapped to the CB05 species based on their carbon bonds, e.g. R4N2 (GEOS's C4-5 alkyl nitrates) can be mapped to NTR + 2.0 PAR in the CB05tucl mechanism. Some of the mapping treatments, such as ALK4 (C4 or higher alkanes) conversion to 4 paraffin carbon bonds (table 2), may have "truncation error" as it only counted butane isomers. However, the effect of this truncation error should be relatively limited for this CONUS LBC influence. The GEOS global model also mainly treats ALK4 as butane or Cn with n ~ 4. Although GEOS's ALK4 emission includes some C5 or higher (C5+) alkanes emission, the relatively shorter lifetime of C5+ alkanes (Helmig et al, 2014) make them hard to reach CONUS from their major upstream source regions, such as East Asia. In this study, wildfire emissions could also contribute certain amount of C5+ alkane on the CONUS LBC, but these C5+ emissions are at least one order of magnitude lower than the corresponding wildfire CO/Ethane/Propane emissions (Urbanski et al, 2008). Again, this species mapping represents an approximation, and the fundamental difference between these two mechanisms for the complex chemistry make the mapping hard to be perfect. In this study, the effect of complex chemistry on the LBC for the pollutant intrusion events (mainly wildfire events) was not significant for the ozone and PM2.5 prediction, since the major

Formatted: Font: (Default) Times New Roman

Formatted: Font: (Default) Times New Roman

Deleted: The corresponding CB05tucl reaction

Deleted: should be

Deleted: Thus we can map GEOS MVK directly into the CB05tucl's ISPD.

wildfire intrusion pollutants from the GEOS global model are CO, NOx, Ethane, Propane, elemental carbon (EC), and organic carbon (OC).

2.2 Aerosol Species Mapping

Both GEOS and NGAC use the GOCART aerosol scheme though in different versions (Bian et al, 2017 and Colarco et al 2010, respectively), and GEOS has additional species of ammonium and 3-bin nitrates (NO3an1, NO3an2 and NO3an3). Table 3 lists the aerosol species mapping from GEOS aerosols to CMAQ Aero6 species used in this study. GEOS aerosols have fixed size bins defined by their diameters, while CMAQ aerosols use 3 size modes: Aitken (ATKN), accumulations (ACC) and coarse (COR) modes (i, j, k modes) (Appel et al., 2010) and each size mode has its own lognormal size distribution (Whitby and McMurry, 1997). To convert the aerosol species from GEOS to CMAQ's Aero6, we need to consider not only the aerosol composition and the conversion from GEOS size bins to the CMAQ size modes, but also the size distribution within each CMAQ size mode that is controlled by the CMAQ aerosol number concentrations (the 3rd column of Table 3). GEOS's dust aerosols are mapped to AOTHRJ (other unreactive aerosols in accumulation mode) and ASOIL (soil particles in coarse mode) in CMAQ. They do not participate in any aerosol reaction, but are only counted in total PM2.5 and PM10. Although the CMAQ Aero6 has explicit elemental ions, like Ca and Mg, which are possible dust ingredients, we do not consider the reaction effect due to these ions. Tang et al. (2004) studied the dust outflow during the ACE-Asia field experiment and found that only a small portion of cations in dust particles are available for aerosol uptake or reactions, which was nearly none for aged dust air masses.

Deleted: Dust
Deleted: is
Deleted: converted
Deleted: just

3. Case Studies for the CLBC in Summer 2015

Deleted: s

To evaluate the impact of the CLBC on the model simulations, we chose the period with pollutant intrusion events. During summer 2015, two intrusion events occurred in the Southeastern USA and Northern USA, respectively. The Southeastern intrusion was brought by the long-range transported dust storm from the Saharan desert. The northern intrusion was caused by the Canadian wildfire and its southward transport into the CONUS. Figure 1 shows the aerosol optical thickness retrieved from Suomi-NPP satellite's VIIRS instrument from later June to early July, 2015, which highlights these two intrusion events.

Deleted: s
Deleted: that covered
Deleted: the
Deleted:

Deleted:

3.1 Dust Storm Events in Summer 2015

As shown in Figure 2, a dust storm originating from the Saharan desert reached the Southeastern USA via the trans-Atlantic transport. The two global models, GEOS and NGAC, captured this dust intrusion, and fed the NAQFC with signals of aerosol increments via their CLBCs. Figure 3 shows the corresponding three LBCs for ASOIL and AOTHRJ along the model's boundary locations on July 2, 2015 as the GOCART dusts have been mapped into two CMAQ aerosol species (Table 3). The base run (CMAQ_BASE) used the clean background for these two CMAQ aerosols. All three LBCs show enhanced ASOIL and AORTHJ near the domain's

Deleted: 1
Deleted: was
Deleted: ed
Deleted: , and brought
Deleted: to
Deleted: provided
Deleted: to NAQFC
Deleted: Figure 2 shows the NAQFC domain and its southeastern corner covered the Bermuda and Bahamas Islands.

southeastern corner and central Southern boundary. The GLBC-Monthly represents the monthly average of GEOS-LBC for July 2015, and has the lowest increments for the two types of aerosols. The two dynamic LBCs, the GEOS-LBC and NGAC-LBC, show the similar aerosol increments over similar locations. However, the NGAC aerosols tended to spread broader than those of the GEOS-LBC, especially for ASOIL, which could reach above the altitude of 10km with concentrations > 5 $\mu g/m^3$ (Figure 3e). The NGAC-LBC also showed some signals over the western boundary, where the GEOS-LBC did not show any dust-related aerosols. Another difference between these two LBCs is their ratio of AORTHJ versus ASOIL. The dynamic NGAC-LBC had the higher ASOIL, the coarse-mode dust, than that of GEOS-LBC (Figure 3a, 3e), but its AOTHRJ (accumulation-mode dust) was lower than the latter (Figure 3b, 3f), especially over the central southern boundary, where the GEOS-LBC had AOTHRJ up to 30 $\mu g/m^3$. It implied that these two global models could have some difference on their dust size distributions, besides their difference on transport patterns due to their dynamics or physics.

Figure 4 shows the regional PM2.5 comparisons with the observations from the U.S.EPA AIRNow stations. The CMAQ_Base represented the clear background situation, which obviously missed this dust intrusion event, and underestimated the PM2.5 over Southern and Southeastern USA. The two dynamical LBCs, GEOS-LBC and NGAC-LBC, well captured the intrusion signals and yielded the best results. Their performance was similar in Florida, which was much better than the CMAQ_BASE, but still underpredicted the PM2.5 over central Florida. Over Texas, the further downwind region of this dust intrusion, the GEOS-LBC yielded broader and higher PM2.5 increments than that of the NGAC-LBC, and agreed better with observations, though it had some overprediction over Northern Texas. The monthly averaged GLBC-Monthly had moderate PM2.5 enhancement and still underestimated the dust intrusion, ranking between the CMAQ_BASE and two dynamic LBCs. Figure 5 shows a similar story for the scenario of 3 days later. The GEOS-LBC yielded the best overall results, though it still underpredicted the PM2.5 over Florida and Northern Texas. Figure 6 illustrates the time-series comparison for this dust intrusion case over Florida and Texas. In general, the performance ranking of these simulations had GEOS-LBC > NGAC-LBC > GLBC-Monthly > CMAQ_Base, except the NGAC-LBC's underprediction over Florida in June. Even though these dynamic LBCs had overall better results than the static LBCs, they still missed some intrusion peaks, such as June 30th over Texas, and had some inconsistent time-variation patterns compared with the observations, e.g. July 1st over Florida, and July 8th over Texas. The two dynamic LBCs had similar performance over Florida in July. However, in the further downwind area, such as Texas, the GEOS-LBC showed better results than that of the NGAC-LBC. These model-observation comparisons showed the advantage of the dynamic LBCs for capturing intrusion events. It should be noted that the PM2.5 spike at night of July 4th (July 5th in UTC time) was not related to the dust intrusion, but caused by firework emissions at night for Independence Day, and that emission was not included in our anthropogenic emission inventory.

Deleted: is

Deleted: were

Deleted: night

Deleted: the

Deleted:

3.2 The Wildfire Event in Summer 2015

During the same period of summer 2015, a wildfire event occurred in Canada and the biomass burning plume was transported to the United States and affected the Northern USA, as shown in Figure 2. Differing from the dust storm intrusion that mainly affected the particle matter (PM) concentrations, the biomass burning plumes also included gaseous pollutants, such as enhanced level of CO, NO_x, and volatile organic compounds (VOCs), which could contribute to the photochemical generation of ozone. For aerosol species, the biomass burning air mass was mainly represented with the enhancement of elemental carbon (EC) and primary organic carbon (POC), or AECJ and APOCJ in CMAQ (Table 3). Figure 7 shows a snapshot of the LBCs along the domain boundaries for AECJ+APOCJ and CO. The GEOS-LBC showed the highest aerosol and CO concentrations with AECJ+APOCJ up to 300 $\mu g/m^3$, and CO up to 3000 ppbV along the domain's northern boundary. Another noticeable feature is that the GEOS-LBC showed CO enhancement appeared at elevated altitudes up to 12km (Figure 7b). The monthly averaged GLBC-monthly showed the similar features to the GEOS-LBC, but with much lower concentrations (Figure 7c, 7d). The NGAC-LBC had the similar AECJ+APOCJ profiles to GLBC-monthly, and it used the static profile CO boundary condition (same as the CMAQ_base) that did not reflect the wildfire influence (Figure 7e, 7f).

As enhanced gaseous pollutants brought by the full-chemistry LBCs would increase the photochemical generation of ozone, the higher ozone also appeared along the northcentral boundary (Figure S1a, S1b), where the GEOS-LBC showed 10 ppbv or higher O_3 concentration than that in the static NGAC-LBC or CMAQ_Base for the altitudes < 4km (Figure S1c). The wildfire induced ozone enhancement appeared not only in the lower troposphere, but also at higher altitudes, e.g. 11km, where the high ozone did not solely come from the stratosphere (Figure S1a). Figure S2 showed the other species from GEOS-LBC, in which the short-lived NOx had less than 1 ppbv increment (Figure S2a) due to the wildfire intrusion. However, its NOz (sum total of all NOx oxidation products, NOz=NOy-NOx) enhancement could reach 30 ppbv (Figure S2b) along the northern boundary around 10-12km altitude, with the co-existed CO increment (Figure 7b). NOz is a good indicator for NOx's photochemical formation of ozone (Sillman et al., 1997) and the O_3/NOz ratio is used as the ozone photochemical efficiency per NOx. The CO and NOz appearance in the high altitudes reflected that the GEOS injected the wildfire emissions to the upper troposphere due to the strong fire plume rise. Besides these species, the VOCs also showed increment due to the wildfire plume, such as ethane (Figure S2c) and HCHO (Figure S2d). HCHO is a short-lived species, and an indicator of VOC oxidation (Arlander et al., 1995). With these magnitudes of CO, VOC and NOx increments, the GEOS-LBC mainly provided the VOC and CO rich airmass with limited NOx to the regional CMAQ model. When this CO/VOC rich airmass arrived at NOx-rich regions, such as the urban areas, it would contribute to the photochemical generation of ozone.

Figure 8 shows the comparison of PM2.5 predictions at 18 UTC, 07/03/2015. The CMAQ_Base missed the intruded biomass burning plumes and the corresponding high PM2.5 over

Deleted: 1
Deleted: were
Deleted: important feature of
Deleted: was that its
Deleted:
Deleted: below 4km more
Deleted: those
Deleted: <
Deleted: be
Deleted: up to
Deleted: where
Deleted: also co-existed
Formatted: Subscript
Deleted: from
Deleted: case
Deleted: Considering
Deleted: in this LBC
Deleted: kind of

North/South Dakoda, Montana, and Minnesota (Figure 8a). The GEOS-LBC predicted the highest PM2.5 increment (up to 200 μg/m^3) over these states, agreed best with the AIRNow observation, though still had some missed predictions, including both underprediction and overprediction (Figure 8b). The dynamic NGAC-LBC and static GLBC-Monthly showed the similar PM2.5 enhancements over the affected states, but were almost one order of magnitude lower than that of GEOS-LBC. Figure 9 showed the similar predictions but for ozone. Again, the GEOS-LBC yielded the highest ozone increment due to its relatively high ozone concentration from the wildfire plume, which, however, still underestimated the ozone over North Dakota (Figure 9b). The monthly mean LBC, GLBC-Monthly, systematically underestimated the ozone over these regions. The CMAQ_Base and NGAC-LBC used the same static gaseous LBC, including that for ozone, and underestimated more. Since the NGAC-LBC had more wildfire-induced aerosol loading than that of CMAQ_Base, the former's photolysis rate was lower than the latter. As both of NGAC-LBC and CMAQ_Base had the "clean" air mass with low-concentration ozone precursors over the Northern USA, the photolysis reduction due to aerosols mainly led to the reduced ozone's photolytic destruction, such as $O_3 \rightarrow O^1D + O_2$ or $O_3 \rightarrow O^3P + O_2$, instead of its photochemical generation. For the same reason, the ozone's lifetime in winter is longer that in summer (Janach, 1989). On the contrary, over polluted regions, the photolysis reduction would cause a lower ozone concentration by limiting its photochemical production. Overall, this effect of photolysis rates on ozone was relatively small. Figure 10 shows the time-series comparison over the Northcentral and Northeastern USA for PM2.5 and ozone. Except the systematic PM2.5 underestimation on the night of July 4th due to the missed firework emissions, the GEOS-LBC showed better PM2.5 prediction than the others, especially from June 29 to July 2 over Northern USA. It should be noted that this run was still not perfect, showing the underestimated PM2.5 in the further downwind, the Northwestern USA. The GEOS-LBC also better captured the peak ozone concentrations, e.g. July 1st and July 2nd, though it sometimes overpredicted ozone, especially during nighttime. The small ozone difference between the CMAQ_Base and NGAC-LBC reflected the impact of wildfire aerosols on photolysis rates, which was very small with regional averages < 1 ppbv throughout this period (Figure 9c, 9d).

3.3 Statistics and Discussion

Table 4 summarizes the PM2.5 statistic results during the two weeks of the intrusion events over the CONUS domain and sub-regions. The dynamic LBCs, GEOS-LBC and NGAC-LBC, showed significant improvements for almost all scores over these regions as compared to the CMAQ_Base. The GLBC-Monthly was also better than the base case, though its improvement on correlation coefficient R and index of agreement (IOA) was relatively moderate compared to the dynamic LBCs, as the time-averaging method removed the temporal variations. Over the further downwind regions of the intrusion events, the LBCs' improvement depended on the regional characteristics of pollutant concentrations. For instance, since the Rocky Mountain region was relatively clean due to its low local PM sources, the external influence weighed more,

Deleted: the
Deleted: and
Deleted: it
Deleted: shows
Deleted: i
Deleted: they
Deleted: carried
Deleted: as it
Deleted: its
Deleted: For

and the LBCs also showed more significant impact there. Over more polluted regions where relatively strong local PM emissions existed, such as Pacific Coast and Northeastern USA, the LBCs mainly changed the background concentration for PM2.5, and had a very limited impact on R or IOA. Overall, the GEOS-LBC yielded the best prediction by reducing the mean bias (MB), root mean square error (RMSE) and increasing the R and IOA. Another dynamic LBC, NGAC-LBC, ranked second. All these LBCs showed better performance than the base case for PM2.5 prediction.

Table 5 shows the similar statistics for ozone. It should be noted that the CMAQ_Base had a systemic O_3 overprediction, especially over the Southcentral region, which affected the improvement of LBCs. Differing from PM2.5, ozone had strong diurnal variation during the summertime, which made the LBCs' impact on R and IOA less significant. It should also be noted that the NGAC-LBC did not change any precursor concentrations related to ozone production, and only affected the ozone formation by reducing photolysis rates. Therefore, as compared to CMAQ_Base, the NGAC-LBC had very weak influence on O_3 and only reduced the regional O_3 by around 0.2 ppbV, and had almost no impact on R or IOA. The GEOS-LBC tended to increase ozone concentrations in most regions, except the Southcentral USA, where the GEOS-LBC showed general improvement for all scores. It had the weakest impact on ozone over Pacific Coast and Rocky Mountain regions, or the farther downstream areas. The GLBC-monthly had the highest ozone increment over most regions except the Southcentral, and also had the slightly higher RMSE. This result showed that removing temporal variation of LBCs might not affect ozone prediction linearly. The GEOS-LBC got better scores except the mean bias over most regions, though the improvement on O_3 was not as significant as that on PM2.5. As discussed above, the LBC's impact on ozone inside the domain was realized through changing inflow concentration of O_3 itself and/or O_3 precursors, such as NOx, VOC or CO. The distance or depth of LBC's effective impact from the inflow boundary depended on the lifetime of these species. All these species have a longer lifetime in winter than those in summer. Our other study showed that the LBC's impact on ozone in winter was stronger than that in summer.

Figure 11 further illustrated the impact of LBCs (using GEOS-LBC as an example) on prediction statistics and their relations to the distance from the domain boundary during the intrusion events: Southern USA for the Saharan dust intrusion (Figure 11 a,b), and Northern USA for the wildfire intrusion case (Figure 11 c, d). As discussed before, the CLBC could have two effects in the regional predictions: provide a constraint for background concentrations, represented by the mean biases, and introduce the dynamic external influence, represented by the correlation coefficients. Both the background and the variation of CLBCs affected the RMSE of predictions. Over the Southern USA, the Saharan dust storm intruded through the states of Texas and Louisiana, or -100°W to -86°W, and moved northward (Figure 4). Figure 11a showed that the GEOS-LBC's improvement on the correlation coefficient R for the PM2.5 prediction reached the highest near the southernmost near-boundary region, and gradually reduced along the latitude for the inland region. On the other hand, the corresponding MB improvement for PM2.5 did not

Deleted: sources
Deleted: their
Deleted: were very limited
Deleted: The
Deleted: just
Deleted: by
Deleted: generally
Deleted: ing
Deleted: its
Deleted: was also slightly higher
Deleted: a
Deleted: Except the mean bias, the
Deleted:
Deleted: has
Deleted: roles
Deleted: variational
Deleted: States
Deleted: ly

show significant reduction along the distance from the influenced boundary. The second effect of CLBCs, constraining background concentrations for PM2.5, can affect farther inside of the domain. The PM2.5 RMSE change reflected the combined changes of MB and R, and the improvement brought by the GEOS-LBC also reduced along the distance from the influenced boundary since the MB improvement did not vary much and the trend of the RMSE change mainly followed the change of R along the latitude. The spatial variations of O_3 statistics differed obviously from those of PM2.5 statistics (Figure 11b), and the most significant R improvement for O_3 was not near boundary, but in some middle latitudes (29°N to 32°N) before being reduced in the farther inland. With the dynamical LBC, the ozone's MB and RMSE improvements had the similar spatial variations, and they were the highest near the boundary and reduced along the latitude increment. One reason for this difference between PM2.5 and O_3 statistics is that the O_3 usually has stronger local diurnal variation in summer driven by the photochemical activities, and that influence on R could be stronger than the external influence over polluted areas. So, for this event in which O_3 was not the key species, the GEOS-LBC's influence on O_3 prediction was mainly about changing O_3 background concentration. Figure 11b also showed that the O_3 MB of the GEOS-LBC run could change from lower to higher than that of the reference run (CMAQ_base) along with the latitudinal increment. Although the ozone concentration of the GEOS-LBC over the south boundary was lower than that of the CMAQ_base in low altitudes, the GEOS-LBC had higher ozone values in the altitudes higher than 14000 m (Figure S1). That high ozone concentration could reach the surface after a certain distance of downward transport in the model system with strong vertical mixing (Tang et al., 2009), which resulted in the higher ozone MB of the GEOS-LBC over the deeper inland region.

For the wildfire intrusion event over Northern USA, the PM2.5 statistical difference between GEOS-LBC and CMAQ_Base showed the similar spatial distribution to the dust intrusion event: the most significant R and RMSE improvements brought by the GEOS-LBC appeared near the boundary, and these improvements reduced along the distance from the boundary. The corresponding MB difference could exist deeper inland (Figure 11c). For the O_3 statistic, the difference between GEOS-LBC and CMAQ_Base became more complex as the wildfire plume also contained the intrusion influence for O_3 and its precursors. The GEOS-LBC run generally yielded higher O_3, which exaggerated the existing overprediction bias near the boundary, but helped correct the underprediction bias when moving farther inland (Figure 11d). The biggest difference of O_3 MB also appeared in the middle latitude as the O_3 precursors brought by the full-chemistry LBC took some time to contribute to O_3 photochemical formation. The spatial variation of O_3 RMSE difference was similar to that of O_3 MB except for the farther inland region with latitude < 43°N where the GEOS-LBC did not improve the RMSE. The similar issue also appeared for the R difference for the region south of 46°N, implying that the wildfire plume represented by the GEOS-LBC could introduce some spatial or temporal biases for O_3 precursors. So, the quality and accuracy of the LBC are important for regional predictions.

Deleted: role
Deleted: the
Deleted: its
Deleted: change
Deleted: R's
Deleted: the
Deleted: reducing
Deleted: Its
Deleted: its
Formatted: Subscript
Deleted: of
Deleted: it
Deleted: of
Deleted: the most significant
Deleted: ,
Deleted: and its
Deleted: be maintained
Deleted:

4. AOT Derived Lateral Boundary Conditions

The dynamic CLBCs, such as GEOS-LBC, showed overall better prediction for the intrusion events by capturing the external influence at right time over right locations. However, this full-chemistry LBC sometimes is not easy to obtain, especially for the near-real-time forecast. Its event-dependent emissions, such as the wildfire emission, also need some time to get relatively accurate estimation, and their impacts on regional domains could lag behind the scene for the forecast. In order to get the intrusion influence when the real-time LBC was not available, we tested the method of developing an alternative LBC based on the historical data with certain indicators. Here we focused on the wildfire intrusion, since it was more difficult to capture the sudden outbreak of wildfire signal than the long-range transport dust intrusion. In addition, the operational NGAC dust forecast has been available to NAQFC (Wang et al, 2018).

4.1 Development of the LBC with VIIRS AOT for Wildfire Plumes

A reliable global-model LBC may not be available in some circumstances, and an alternative method is needed for this situation. Here we developed and tested an indicator-derived LBC. AIRNow surface stations could be such an indicator, as these surface data are reliable and in hourly resolution. However, their spatial coverage along the wildfire intrusion boundary (north boundary) is not dense enough for this purpose. Figure 2 showed that the VIIRS retrieved AOT well reflected the wildfire intrusion with broad spatial coverage, superior to the sporadic surface stations along the north boundary of the CONUS domain. So VIIRS AOT could be used as an indicator for wildfire plumes. Figure S3 showed the comparison of extracted VIIRS AOT versus GEOS CO and EC column loading along the northern boundary for June-July, 2015, with their correlation coefficients $R > 0.5$. The regression relationship derived out of Figure S3 can then be used to resample the historical GEOS-LBC data to derive a new LBC for wildfire intrusion events when the corresponding AOT is available. The domain's northern boundary was relatively clean in most periods of the summer, unless the wildfire events occurred. During the June and July 2015, the VIIRS AOT data was available once or twice per day around local noontime under cloud-free condition. To get more VIIRS AOT data along the northern boundary, we relaxed the influencing distance up to 300 km when pairing the VIIRS AOT geolocation and the northern boundary location with the nearest neighbor method. In this study, we paired the GEOS's northern LBC (NLBC) for 18UTC with the daily VIIRS AOT along the same location, and made an average of the whole column with AOT interval of 0.2 to build a LBC database sorted in AOT. We only chose to resample the LBC for primarily emitted species from the wildfire sources, including POC, EC, CO, NOx, and two NOz species: PAN and HNO_3, but did not include the ozone LBC. When the VIIRS AOT for the new events are available for NLBC, the whole-column species concentration data from that database are chosen to form the new LBC based on the VIIRS AOT value in the nearest neighbor.

Deleted: depended

Deleted: 1

Deleted: GEOS

Deleted: time

4.2 A Case Study with VIIRS AOT Derived LBC in August, 2018

In the middle-later August 2018, a wildfire occurred in western Canada. Figure S4 showed that there was a high-pressure system with peak surface pressure up to 1022 hPa in the western Canada, and the dry weather made the wild fire easily spread. There was prevailing northern or northeastern wind, which brought the fire pollutants southward to affect the northwestern and northern U.S. states. Figure 12a shows the VIIRS AOT for this event with the high AOT appearing in the western Canada, the main source region, and the Northern and Northwestern USA. We used this AOT data to derive the new LBC along the northern boundary (Figure 12b, c) for CO and wildfire emitted aerosols (AECJ+APOCJ) by resampling the historical GEOS-LBC database from the Jun-Jul, 2015 period. This AOT derived northern LBC (AOT-NLBC) was updated once per day due to the VIIRS data availability, while its western, southern, and eastern boundaries came from the climatological monthly-mean GEOS-LBC (averaged from 2011 to 2015). The AECJ+APOCJ increment of the AOT-NLBC mainly existed below 3km, but its CO enhancement could reach up to the altitude of 10km, due to the elevated CO plume in the original GEOS-LBC, e.g. Figure 7b. The NGAC-LBC (Figure 13d) also showed the enhanced AECJ+APOCJ concentrations along the north boundary, but it was much lower than that of AOT-NLBC. Also, unlike the AOT-NLBC's two peaks, the NGAC-LBC mainly just showed one peak near the northwest boundary.

Figure 13 shows the surface ozone and PM2.5 over this region one day later (08/17/2018). The CMAQ_Base underpredicted both species over this region, and the AOT-NLBC reduced the underprediction with increased background concentration from the northern boundary. Since the AOT-NLBC did not include the dynamic ozone boundary condition, the enhanced ozone concentration was mainly brought by the CO and NOx increments from the northern boundary, which sometimes caused the overprediction over further downwind areas, such as North Dakota. Overall, the AOT-NLBC showed better PM2.5 prediction over Southwestern Canada and Northwestern USA with its higher background concentrations. The NGAC-LBC yielded almost the same ozone concentration as that of the CMAQ_Base (Figure 13e), and had similar PM2.5 background enhancement to that of the AOT-NLBC over Northwestern USA. Unlike the AOT-NLBC, the NGAC-LBC did not show PM2.5 increment in east of -96°W compared to the CMAQ_base run, as the AOT-NLBC had additional aerosol incremental peak over the domain's north central boundary. However, that aerosol background increment of the AOT-NLBC led to the PM2.5 overprediction over Minnesota, implying that the derived LBC could bring errors.

Figure 14 shows the corresponding time-series comparison over EPA region 8 (states of Montana, North and South Dakotas, Wyoming, Colorado, and Utah), region 10 (states of Washington, Idaho, and Oregon), region 5 (states of Minnesota, Wisconsin, Illinois, Indiana, Michigan, and Ohio) and region 8 (states of California, Nevada and Arizona). Both observed and predicted ozone showed strong diurnal variation. The AOT-NLBC showed better skill on capturing daytime ozone maximum for the region 8 and 10, and was about 3-10 ppbv higher than the CMAQ_base prediction, though it tended to overpredict ozone at night. Over the EPA region

Deleted:

Deleted: a

Deleted: controlled

Deleted: to

Deleted: were

Deleted: climatologic

Deleted: while

Deleted: greatly

Deleted: LBC

Deleted: its

Deleted: Colorado

Deleted: Dokotas

Deleted: and

Deleted: 5

Deleted: , especially over the region 8

5 (north central USA), the ozone difference between the AOT-NLBC and CMAQ_base runs became narrower as the major pollutant intrusion of this event occurred in the northwestern USA. The AOT-NLBC increased the existing ozone high bias over the region 5. The region 9 (Southwestern USA) was located in further downwind from the domain's north boundary, which should get much weaker influence from the AOT-NLBC. However, during a certain period (08/21-08/25/2018), the impact of the AOT-NLBC on ozone could still reach about 5 ppb, and the derived LBC generally improved the ozone prediction scores over that region. It implies that the long-lived wildfire pollutant, such as CO, could be transported to the farther downwind, and had an impact on ozone. Throughout this period, the ozone difference between the NGAC-LBC and CMAQ_Base was very small, mainly caused by the aerosol effect on the photolysis.

For PM2.5, the CMAQ_Base run had systemic underprediction for all the 4 EPA regions in Figure 14, especially over the region 10, as the northwestern states encountered the major wildfire inflow. The AOT-NLBC and NGAC-LBC improved the predictions by narrowing the mean bias up to 10 $\mu g/m^3$, over the region 10 (Figure 14d), though still underpredicted PM2.5. These two dynamic LBCs had similar performance over the northern states, or the regions 8, 10, and 5. In the region 9, they showed some difference for their temporal variation (Figure 14h) as the AOT-NLBC only changed the north boundary. The AOT-NLBC ovepredicted PM2.5 during 08/21- 08/23/2018, and the NGAC-LBC yielded higher PM2.5 after 08/25 over the region 9. Even though the AOT-NLBC only changed the north boundary, that LBC could influence the whole domain during the intrusion events. The domain-wide statistics of surface PM2.5 prediction are R=0.39, 0.45, 0.50; MB=-7.53, -2.33, -2.70; RMSE=25.12, 24.04, 22.93 for the CMAQ_Base, NGAC-LBC, and AOT-NLBC runs, respectively. The AOT-NLBC had the best overall scores, except that the NGAC-LBC had slightly better mean bias with its dynamically changed four boundaries.

This result showed that the alternative LBC could be useful for capturing the key intrusion signals in case the global LBC was not available. This alternative approach was especially important for the forecast as the satellite AOT can be obtained in near-real-time. In this case study of summer 2018, the wildfire events were similar to the wildfire cases that occurred in summer 2015, which made the quantitative derivation of LBC possible. However, this method may also bring some biases, which could be due to two reasons. One reason is that the correlation shown in Figure S3 is not very strong and some value discrepancies may exist in the derivation. Another reason is that either AOT or the total column loading of pollutants does not include any vertical distribution information, but depends on the based database of summer 2015, in which the major aerosol intrusion occurred below 3km (Figure 7). If the new events had major elevated aerosol signals, the AOT derived LBC could put too many aerosol in lower layers and cause surface PM2.5 overprediction.

Deleted: observation clearly showed two peaks related to wildfire plumes over two regions: 08/19-08/21 and 08/24-08/25 for EPA region 8; 08/14-08/17 and 08/19-08/22 for EPA region 10. Without the boundary influence, the CMAQ_Base missed all these PM2.5 peaks even though it had the same inside-domain wildfire emissions.

Deleted: successfully captur

Deleted: these

Formatted: Superscript

Deleted: intrusion signals

Deleted: ,

Deleted: overpredicted

Deleted:

Deleted: before 08/18 over EPA region 8

Deleted: alterative

Deleted:

Deleted:

5. Conclusion

In this study, we examined the influence of CLBCs on our regional air quality prediction, verified with surface ozone and PM2.5 monitoring observations. We developed the full-chemistry mapping table from the global model GEOS to CMAQ's CB05-Aero6 species. The GEOS dynamic LBC showed the overall best score compared with the surface observations during June-July 2015 when the Saharan dust intrusion and Canadian wildfire events occurred. The base simulation (CMAQ_Base) ranked last as it missed all these external influences. The NGAC-LBC only considered the GOCART aerosols, and had the good performance for capturing the dust storm intrusion but missed the ozone enhancement due to the Canadian fire events. The LBC's influences on the model performance depended on not only the distance from the inflow boundary but also species and their regional characteristics, as the LBCs' influence on ozone and PM2.5 differed significantly. During the studied events of summer 2015, The CLBCs affected both PM2.5 mean background concentration and its temporal/spatial variation. Their influences on PM2.5's correlation coefficient R mainly appeared near the inflow boundary, and reduced along with the distance from the boundary. However, their influence on PM2.5 background concentration could be kept in the farther inside domain. The CLBC influence on ozone could be more complex, and affected by the boundary inflow of ozone and/or its precursors, and downward transport from the upper troposphere. In this study, the influences with temporal/spatial variation were mainly shown in the aerosol dynamic LBC, e.g. the GEOS-LBC or NGAC-LBC. All other LBCs mainly changed the background concentrations and shifted the mean bias of the corresponding predictions. It should be noted that this study mainly focused on the CLBCs influence on surface sites. For elevated locations, such as airborne measurements, the temporal/spatial variation of the CLBCs can also affect ozone due to the relatively fast transport and weak local ozone production in the upper layers (Tang et al., 2007)

The AOT-derived LBC can be used as an alternative method to capture the intrusion when a reliable dynamic LBC is not available. Although the VIIRS AOT was updated only once per day and the derived LBC had noisy spatial distribution, this method still showed its value to replace the static LBC in the air quality forecast. In the wildfire intrusion events of summer 2018, the AOT-derived LBC showed better scores than the NGAC-LBC. Using this derivation method needs some cautions as it could bring some biases due to the value discrepancy or inconsistent vertical distribution between the new event and the original events used to make the derivation. It should be noted that other indicators, such as surface monitoring data, can be also used to derive the similar LBC if the historical LBC has good correlation with these data and there are relatively dense stations available near the inflow boundary. Geostationary satellites can achieve a near-real-time AOT retrieval in a time interval of several minutes, which will provide a better solution for fast capturing the intrusion signals. Currently the main issue for using geostationary AOT is their relatively poor retrieval quality over high latitude or under high zenith angles. Once that issue gets resolved, its AOT can be used as an indicator to derive the LBC or even replace the LBC provided by the global models.

Deleted: the C

Deleted: when comparing

Deleted: the

Deleted: while

Deleted: further

Deleted: s'

Deleted:

Deleted:

Code and Data availability

The source code used in this study is available online at https://github.com/NOAA-EMC/EMC_aqfs (last access: 4 May 2020; NOAA-EMC, 2020). The VIIRS AOT data used here are in ftp://ftp.star.nesdis.noaa.gov/pub/smcd/VIIRS_Aerosol/npp.viirs.aerosol.data/epsaot550/. The surface AIRNow monitoring data can be obtained via https://airnow.gov.

Acknowledgements

This research was supported by National Oceanic and Atmospheric Administration (NOAA) under its Office of Weather and Air Quality program with funding number NA16OAR4590118 and NOAA National Air Quality Forecast Capability (grant # T8MWQAQ). We thank the NASA MAP program and NASA Center for Climate Simulation for support in of the GEOS GMI model.

Reference

Appel, K. W., S. J. Roselle, R. C. Gilliam, and J. E. Pleim, Sensitivity of the Community Multiscale Air Quality (CMAQ) model v4. 7 results for the eastern United States to MM5 and WRF meteorological drivers. Geosci. Model Dev., 3, 169–188, 2010.

Arlander, D.W., Brüning, D., Schmidt, U. and Ehhalt, D.H., 1995. The tropospheric distribution of formaldehyde during TROPOZ II. Journal of atmospheric chemistry, 22(3), pp.251-269.

Bey, I., D.J. Jacob, J.A. Logan, R.M. Yantosca, Asian chemical outflow to the Pacific in spring: origins, pathways, and budgets. *J. Geophys. Res.*, 106 (D19), pp. 23097-23113, 2001.

Bian, H., M. Chin, D. A. Hauglustaine, M. Schulz, G. Myhre, S. E. Bauer, M. T. Lund, V. A. Karydis, T. L. Kucsera, X. Pan, A. Pozzer, R. B. Skeie, S. D. Steenrod, K. Sudo, K. Tsigaridis, A. P. Tsimpidi, and S. G. Tsyro (2017), Investigation of global particulate nitrate from the AeroCom phase III experiment Atmos. Chem. Phys., 17, 12911–12940 (https://www.atmos-chem-phys.net/17/12911/2017/).

Chin, M., Rood, R. B., Lin, S.-J., Muller, J.-F., and Thompson, A. M.: Atmospheric sulfur cycle simulated in the global model GOCART: Model description and global properties, *J. Geophys. Res.*, 105, 24671–24687, doi:10.1029/2000JD900384, 2000.

Chin, M., Ginoux, P., Kinne, S., Torres, O., Holben, B. N., Duncan, B. N., Martin, R. V. , Logan, J. A., and Higurashi, A.: Tropospheric aerosol optical thickness from the GOCART model and comparisons with satellite and Sun photometer measurements, *J. Atmos. Sci.*, 59, 461–483, 2002.

Colarco, P., da Silva, A., Chin, M., Diehl, T., Online simulations of global aerosol distributions in the NASA GEOS-4 model and comparisons to satellite and ground- based aerosol optical depth. J. Geophys. Res. 115, D14207. https://doi.org/10.1029/2009JD012820. 2010.

Eastham, S.D., Weisenstein, D.K. and Barrett, S.R., Development and evaluation of the unified tropospheric–stratospheric chemistry extension (UCX) for the global chemistry-transport model GEOS-Chem. Atmospheric Environment, 89, pp.52-63. http://dx.doi.org/10.1016/j.atmosenv.2014.02.001, 2014.

Deleted:

Foley, K. M., Roselle, S. J., Appel, K. W., Bhave, P. V., Pleim, J. E., Otte, T. L., Mathur, R., Sarwar, G., Young, J. O., Gilliam, R. C., Nolte, C. G., Kelly, J. T., Gilliland, A. B., and Bash, J. O.: Incremental testing of the Community Multiscale Air Quality (CMAQ) modeling system version 4.7, Geosci. Model Dev., 3, 205–226, https://doi.org/10.5194/gmd-3-205-2010, 2010.

Helmig, D., Petrenko, V., Martinerie, P., Witrant, E., Rockmann, T., Zuiderweg, A., Holzinger, R., Hueber, J., Thompson, C., White, J.W.C. and Sturges, W., Reconstruction of Northern Hemisphere 1950-2010 atmospheric non-methane hydrocarbons. Atmospheric chemistry and physics, 14(3), pp.1463-1483, doi:10.5194/acp-14-1463-2014, 2014.

Henderson, B. H., Akhtar, F., Pye, H. O. T., Napelenok, S. L., and Hutzell, W. T.: A database and tool for boundary conditions for regional air quality modeling: description and evaluation, Geosci. Model Dev., 7, 339–360, https://doi.org/10.5194/gmd-7-339-2014, 2014.

Janach, W.E., 1989. Surface ozone: trend details, seasonal variations, and interpretation. *Journal of Geophysical Research: Atmospheres*, 94(D15), pp.18289-18295.

Lee, P., J. McQueen, I. Stajner, J. Huang, L. Pan, D. Tong, H.-C. Kim, Y. Tang, S. Kondragunta, and M. Ruminski, NAQFC developmental forecast guidance for fine particulate matter (PM2. 5), Weather and Forecasting, 32: 343-60. doi:10.1175/waf-d-15-0163.1, 2017.

Lu, C.-H., da Silva, A., Wang, J., Moorthi, S., Chin, M., Colarco, P., Tang, Y., Bhattacharjee, P. S., Chen, S.-P., Chuang, H.-Y., Juang, H.-M. H., McQueen, J., and Iredell, M.: The implementation of NEMS GFS Aerosol Component (NGAC) Version 1.0 for global dust forecasting at NOAA/NCEP, *Geosci. Model Dev.*, 9, 1905-1919, https://doi.org/10.5194/gmd-9-1905-2016, 2016.

Molod, A., L. Takacs, M. Suarez, J. Bacmeister, I.-S. Song, and A. Eichmann, The GEOS Atmospheric General Circulation Model: Mean Climate and Development from MERRA to Fortuna. Technical Report Series on Global Modeling and Data Assimilation, 28, 2012.

Pan, L., Tong, D., Lee, P., Kim, H.C. and Chai, T.. Assessment of NOx and O_3 forecasting performances in the US National Air Quality Forecasting Capability before and after the 2012 major emissions updates. *Atmospheric Environment*, 95, pp.610-619, 2014.

Pan, L., Kim, H., Lee, P., Saylor, R., Tang, Y., Tong, D., Baker, B., Kondragunta, S., Xu, C., Ruminski, M. G., Chen, W., Mcqueen, J., and Stajner, I.: Evaluating a fire smoke simulation algorithm in the National Air Quality Forecast Capability (NAQFC) by using multiple observation data sets during the Southeast Nexus (SENEX) field campaign, Geosci. Model Dev., 13, 2169–2184, https://doi.org/10.5194/gmd-13-2169-2020, 2020

Pierce, T., C. Geron, L. Bender , R. Dennis, G. Tonnesen, and A. Guenther A, Influence of increased isoprene emissions on regional ozone modeling. *J. Geophys. Res.* 103:25611–25629, 1998.

Mathur, R., Xing, J., Gilliam, R., Sarwar, G., Hogrefe, C., Pleim, J., Pouliot, G., Roselle, S., Spero, T.L., Wong, D.C. and Young, J., Extending the Community Multiscale Air Quality (CMAQ) modeling system to hemispheric scales: overview of process considerations and initial applications. Atmospheric chemistry and physics, 17, p.12449. doi: 10.5194/acp-17-12449-2017, 2017

Sarwar, G., Luecken, D., and Yarwood, G.: Chapter 2.9 Developing and implementing an updated chlorine chemistry into the community multiscale air quality model, in: Air Pollution Modeling and Its Application XVIII, edited by: Borrego, C. and Renner, E., vol. 6 of Developments in Environmental Science, 168– 176, Elsevier, Amsterdam, the Netherlands, doi:10.1016/S1474- 8177(07)06029-9, 2007.

Sillman, S., He, D., Cardelino, C. and Imhoff, R.E., The use of photochemical indicators to evaluate ozone-NOx-hydrocarbon sensitivity: Case studies from Atlanta, New York, and Los Angeles. *Journal of the Air & Waste Management Association*, 47(10), pp.1030-1040, 1997.

Sonntag, D. B., R. W. Baldauf, C. A. Yanca and C. R. Fulper, Particulate matter speciation profiles for light-duty gasoline vehicles in the United States, *Journal of the Air & Waste Management Association*, 64:5, 529-545, DOI:10.1080/10962247.2013.870096, 2014.

Strode S.A., J.R. Ziemke, L.D. Oman, L.N. Lamsal, M.A. Olsen, J. Liu, Global changes in the diurnal cycle of surface ozone, *Atmospheric Environment*, 199, 323-333, https://doi.org/10.1016/j.atmosenv.2018.11.028, 2019.

Tanaka, P. L., Allen, D. T., McDonald-Buller, E. C., Chang, S., Kimura, Y., Mullins, C. B., Yarwood, G., and Neece, J. D.: Development of a chlorine mechanism for use in the carbon bond IV chemistry model, *J. Geophys. Res.-Atmos.*, 108, 4145, doi:10.1029/2002JD002432, 2003.

Tang Y., Carmichael G. R., Thongboonchoo N., Chai T., Horowitz L.W., Pierce R. B., Al-Saadi J. A., Pfister G., Vukovich J. M., Avery M. A., Sachse G. W., Ryerson T. B., Holloway J. S., Atlas E. L., Flocke F. M., Weber R. J., Huey L. G., Dibb J. E., Streets D. G., and Brune W. H.: Influence of lateral and top boundary conditions on regional air quality prediction: a multiscale study coupling regional and global chemical transport models. *J. Geophys. Res.* 112:D10S18. doi:10.1029/2006JD007515, 2007.

Tang, Y., Lee, P., Tsidulko, M., Huang, H.C., McQueen, J.T., DiMego, G.J., Emmons, L.K., Pierce, R.B., Thompson, A.M., Lin, H.M. and Kang, D.: The impact of chemical lateral boundary conditions on CMAQ predictions of tropospheric ozone over the continental United States. *Environmental Fluid Mechanics*, 9(1), pp.43-58, DOI:10.1007/s10652-008-9092-5, 2009

Tyndall, G. S., Cox, R. A., Granier, C., Lesclaux, R., Moortgat, G. K., Pilling, M. J., Ravishankara, A.R. and Wallington, T. J.: Atmospheric chemistry of small organic peroxy radicals. Journal of Geophysical Research: Atmospheres, 106(D11), pp.12157-12182, 2001

Urbanski, S.P., Hao, W.M. and Baker, S., Chemical composition of wildland fire emissions. Developments in environmental science, 8, pp.79-107. DOI:10.1016/S1474-8177(08)00004-1. 2008

Wang, J., Bhattacharjee, P.S., Tallapragada, V., Lu, C.H., Kondragunta, S., da Silva, A., Zhang, X.Y., Chen, S.P., Wei, S.W., Darmenov, A.S. and McQueen, J.: The implementation of NEMS GFS Aerosol Component (NGAC) Version 2.0 for global multispecies forecasting at NOAA/NCEP-Part 1: Model descriptions. Geosci. Model Dev., 11, 2315–2332, https://doi.org/10.5194/gmd-11-2315-2018, 2018

Whitby, E. R., and P. H. McMurry, Modal aerosol dynamics modeling. Aerosol Science and Technology 27: 673-688, 1997

Whitten, G. Z., Heo, G., Kimura, Y., McDonald-Buller, E., Allen, D. T., Carter, W. P., and Yarwood, G.: A new condensed toluene mechanism for Carbon Bond: CB05-TU, *Atmos. Environ.*, 44, 5346–5355, doi:10.1016/j.atmosenv.2009.12.029, 2010.

Yarwood, G., S. Rao, M. Yocke, and G. Whitten. Updates to the Carbon Bond Chemical Mechanism: CB05, Technical Report RT-0400675 ENVIRON International Corporation Novato, CA, USA. 2005.

Table 1 . The runs with different lateral boundary conditions conducted in this study

Runs	Aerosol LBC	Gaseous LBC	Temporal Resolution
CMAQ_Base	static clean background	static GEOS-Chem 2006 with O_3 limit ≤ 100 ppbV	static monthly mean
GEOS-LBC	dynamic full aerosol	dynamic full chemistry	3 hours
GLBC-Monthly	monthly mean full aerosol	monthly mean full chemistry	static monthly mean
NGAC-LBC	dynamic GOCART simple aerosol	Same as CMAQ_Base	3 hours
AOT-NLBC	daily AOT derived Northern LBC (NLBC) for EC and POC	daily AOT derived Northern LBC for CO, NOx, PAN, and HNO_3	24 hours for derived NLBC; static monthly mean for all others

Deleted: CLBC

Formatted Table

Deleted: GEOS-Chem 2006 with O_3 limit ≤ 100 ppbV

Table 2. VOC species mapping table from GEOS to CMAQ CB05tucl

GEOS species (mole)	CMAQ Species (mole)
HCOOH	FACD
MO_2 (CH_3O_2)	XO_2
MP (methylhydroperoxide)	MEPX
A_3O_2 (primary RO_2 from C_3H_8: $CH_3CH_2CH_2OO$)	PAR + XO_2
ACTA (acetic acid)	AACD
ATO_2 (RO_2 from acetone: $CH_3C(O)CH_2O_2$)	2*PAR + XO_2
B_3O_2 (secondary RO_2 from C_3H_8: $CH_3CH(OO)CH_3$)	2*B_3O_2
ALK4 (C_4 or higher alkanes)	4*PAR
C_3H_8	1.5*PAR + NR
ETO_2 (ethylperoxy radical: CH_3CH_2OO)	MEO_2 + PAR
ETP (ethylhydroperoxide: CH_3CH_2OOH)	MEPX + PAR
GCO_3 (hydroxy peroxyacetyl radical: $HOCH_2C(O)OO$)	C_2O_3
GLYX (glyoxal)	FORM + PAR
GLYC (glycolaldehyde: $HOCH_2CHO$)	FORM + 2*PAR
GP (peroxide from GCO_3: $HOCH_2C(O)OOH$)	ROOH
GPAN (Peroxyacylnitrate: $HOCH_2C(O)OONO_2$)	PANX
HAC (hydroxyacetone: $HOCH_2C(O)CH_3$)	2*PAR
IALD (hydroxy carbonyl alkenes from isoprene)	ISOPX
IAO_2 (RO_2 from isoprene oxidation products)	$ISOPO_2$
IAP (peroxide from IAO_2)	ROOH
INO_2 (RO_2 from ISOP+NO_3)	0.2*ISPD + 0.8*NTR+ XO_2 + 0.8*HO_2 + 0.2*NO_2 + 0.8*ALDX + 2.4*PAR'
INPN (peroxide from INO_2)	0.2*ISPD + 0.8*NTR+ ROOH + 0.8*H_2O_2 + 0.2*PNA + 0.8*ALDX + 2.4*PAR
ISN1 (RO_2 from isoprene nitrate)	NTRI
ISNP (peroxide from ISN1)	$NTRIO_2$
KO_2 (RO_2 from C_3 or higher ketones)	XO_2 + PAR
MACR (methacrolein)	ISPD
MAN2 (RO_2 from MACR+NO_3)	0.925*HO_2 + 0.075*XO_2
MAO_3 (peroxyacyl from MVK and MACR)	$MACO_3$
MAOP (peroxide from MAO_3)	ISPD
MAP (peroxyacetic acid, $CH_3C(O)OOH$)	PACD
MCO_3 (peroxyacetyl radical)	C_2O_3
MEK (C_3 or higher ketones)	4*PAR
MRO_2 (RO_2 from MACR+OH)	0.713*XO_2 + 0.503*HO_2
MRP (Peroxide from MRO_2)	ROOH
MVK (methylvinylketone)	ISPD
MVN2 (RO_2 from MVK+NO_3)	0.925*HO_2 + 0.075*XO_2
PMN (peroxymethacryloyl nitrate)	OPEN

PO_2 (RO_2 from propene)	XO_2
PP (peroxide from PO_2: HOC_3H_6OOH)	ROOH
PPN (peroxypropionyl nitrate)	PANX
PRN1 (RO2 from propene+NO_3)	XO_2
PRPE (propene)	OLE + PAR
PRPN (peroxide from PRN1)	ROOH
R4N1 (RO_2 from C_4 and C_5 alkylnitrates)	ROOH + 2*PAR
R4O2 (RO_2 from C_4 alkane)	XO_2
R4P (peroxide from R4O2)	ROOH
RA3P (peroxide from A_3O_2)	ROOH
RB3P (Peroxide from B_3O_2)	ROOH
RCHO (C_3 or higher aldehydes)	ALDX
RCO3 (peroxypropionyl radical: $CH_3CH_2C(O)OO$)	XO_2
RCOOH (C_2 or higher organic acids)	AACD
RIO1 (RO_2 from isoprene oxidation products)	ISPD
RIO2 (RO_2 from isoprene)	$ISOPO_2$
RIP (Peroxide from RIO_2)	ISOPX
ROH (C_2 or higher alcohols)	3*PAR
RP (peroxide from RCO_3)	ROOH
VRO_2 (RO_2 from MVK+OH)	$ISOPO_2$
VRP (peroxide from VRO_2)	ROOH
ACET (acetone)	3*PAR

Table 3. Aerosol species mapping table from GEOS to CMAQ Aero6 ("D" represents the diameter of GEOS aerosol bin)

GEOS Aerosol (μg/m^3)	**CMAQ Aerosol Mass Concentration (μg/m^3)**	**CMAQ Aerosol Number Concentration (#/m^3)**
BCPHILIC	AECJ	2.72×10^7 (ACC)
BCPHOBIC	AECJ	2.72×10^7 (ACC)
OCPHILIC	APOCJ	2.72×10^7 (ACC)
OCPHOBIC	APOCJ	2.72×10^7 (ACC)
SO4	ASO4J	2.72×10^7 (ACC)
NH4a	ANH4J	2.72×10^7 (ACC)
NO3an1 (mean D=0.5μm)	ANO3J	2.72×10^7 (ACC)
NO3an2 (mean D=4.2μm)	0.8*ANO3J + 0.2 *ANO3K	5.4×10^6(ACC) + 1.2×10^4(COR)
NO3an2 (mean D=15μm)	ANO3K	6×10^3(COR)
DU001 (D: 0.2 – 2 μm)	AOTHRJ	2.72×10^7 (ACC)
DU002 (D: 2 – 3.6 μm)	0.45*AOTHRJ+0.55*ASOIL	3.3×10^5 (ACC)+5.1×10^4(COR)
DU003 (D: 3.6 – 6 μm)	ASOIL	1.15×10^4(COR)
DU004 (D: 6 – 12 μm)	0.75*ASOIL	1.4×10^3(COR)
SS001 (D: 0.06-0.2 μm)	0.39*ANAI+0.61*ACLI	7.4×10^8(ATKN)
SS002 (D: 0.2 - 1μm)	0.39*ANAJ+0.61*ACLJ	2.72×10^7 (ACC)
SS003 (D: 1- 3μm)	0.312*ANAJ+0.488*ACLJ +0.078*ASEACAT+0.122*ACLK	1.7×10^5(ACC)+1.26×10^4(COR)
SS004 (D: 3- 10μm)	0.39*ASEACAT+0.61*ACLK	1.36×10^4 (COR)

Table 4. Regional $PM_{2.5}$ statistic of the 4 simulations (CMAQ_BASE, GEOS-LBC, GLBC-Monthly and NGAC-LBC) from June 24 to July 8, 2015.

Regions	Simulations	Mean Bias ($\mu g/m^3$)	Root Mean Square Error ($\mu g/m^3$)	Correlation Coefficient, R	Index of Agreement
CONUS	CMAQ_BASE	-6.74	13.69	0.18	0.37
	GEOS-LBC	-2.96	12.16	0.37	0.55
	GLBC-Monthly	-4.10	12.39	0.27	0.41
	NGAC-LBC	-3.30	12.09	0.30	0.44
Northeastern USA	CMAQ_BASE	-5.52	10.93	0.33	0.43
	GEOS-LBC	-3.81	9.89	0.40	0.50
	GLBC-Monthly	-4.25	10.31	0.34	0.45
	NGAC-LBC	-3.70	10.05	0.35	0.46
Pacific Coast	CMAQ_BASE	-3.96	10.63	0.16	0.31
	GEOS-LBC	-2.02	10.22	0.18	0.34
	GLBC-Monthly	-1.53	10.21	0.17	0.34
	NGAC-LBC	-0.79	10.33	0.16	0.34
Southeastern USA	CMAQ_BASE	-8.18	11.35	0.14	0.44
	GEOS-LBC	-3.07	8.39	0.37	0.58
	GLBC-Monthly	-4.78	9.08	0.27	0.49
	NGAC-LBC	-3.83	8.58	0.35	0.56
Rocky Mountain States	CMAQ_BASE	-7.62	17.57	0.02	0.31
	GEOS-LBC	-3.66	15.98	0.39	0.58
	GLBC-Monthly	-5.42	16.06	0.23	0.36
	NGAC-LBC	-4.65	15.78	0.24	0.36
North Central	CMAQ_BASE	-8.32	17.63	0.25	0.38
	GEOS-LBC	-2.95	16.47	0.33	0.52
	GLBC-Monthly	-5.25	16.41	0.27	0.40
	NGAC-LBC	-4.48	15.98	0.31	0.43
South Central	CMAQ_BASE	-9.65	13.12	0.07	0.42
	GEOS-LBC	-2.00	7.79	0.51	0.69
	GLBC-Monthly	-4.73	9.45	0.24	0.48
	NGAC-LBC	-3.52	8.31	0.46	0.63

Table 5. Same as Table 4 but for ozone

Regions	Simulations	Mean Bias (ppbV)	Root Mean Square Error (ppbV)	Correlation Coefficient, R	Index of Agreement
CONUS	CMAQ_BASE	2.10	12.35	0.64	0.77
	GEOS-LBC	3.47	12.01	0.68	0.79
	GLBC-Monthly	4.84	12.52	0.68	0.78
	NGAC-LBC	1.88	12.29	0.64	0.77
Northeastern USA	CMAQ_BASE	1.87	10.68	0.66	0.78
	GEOS-LBC	4.88	11.54	0.68	0.78
	GLBC-Monthly	5.60	12.02	0.66	0.76
	NGAC-LBC	1.62	10.64	0.66	0.78
Pacific Coast	CMAQ_BASE	-2.58	12.04	0.78	0.86
	GEOS-LBC	-2.16	11.83	0.79	0.87
	GLBC-Monthly	0.46	11.79	0.78	0.87
	NGAC-LBC	-2.76	12.08	0.78	0.86
Southeastern USA	CMAQ_BASE	7.26	13.66	0.59	0.68
	GEOS-LBC	7.94	13.34	0.66	0.72
	GLBC-Monthly	9.06	14.20	0.65	0.70
	NGAC-LBC	7.04	13.50	0.60	0.69
Rocky Mountain States	CMAQ_BASE	-1.91	10.61	0.67	0.80
	GEOS-LBC	-0.17	10.45	0.67	0.80
	GLBC-Monthly	1.68	10.75	0.66	0.79
	NGAC-LBC	-2.08	10.63	0.67	0.80
North Central	CMAQ_BASE	-0.47	10.78	0.65	0.78
	GEOS-LBC	2.55	11.01	0.66	0.79
	GLBC-Monthly	3.00	11.22	0.65	0.78
	NGAC-LBC	-0.75	10.76	0.65	0.78
South Central	CMAQ_BASE	13.36	17.76	0.51	0.58
	GEOS-LBC	10.90	14.71	0.68	0.68
	GLBC-Monthly	12.66	16.24	0.66	0.64
	NGAC-LBC	13.12	17.56	0.51	0.58

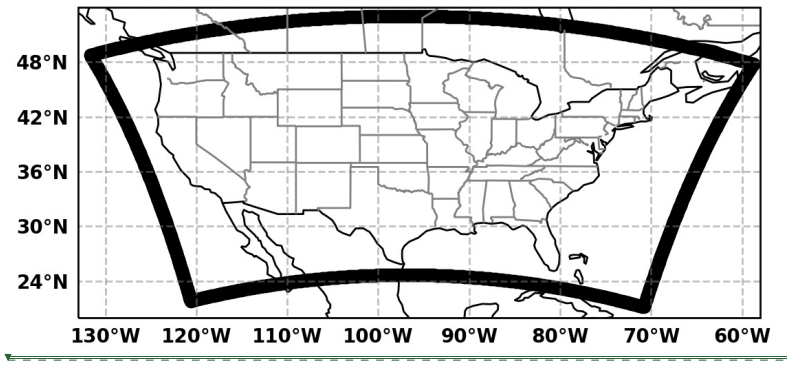

Figure 1. NAQFC CONUS domain (bold black)

Moved (insertion) [1]

Deleted: 2

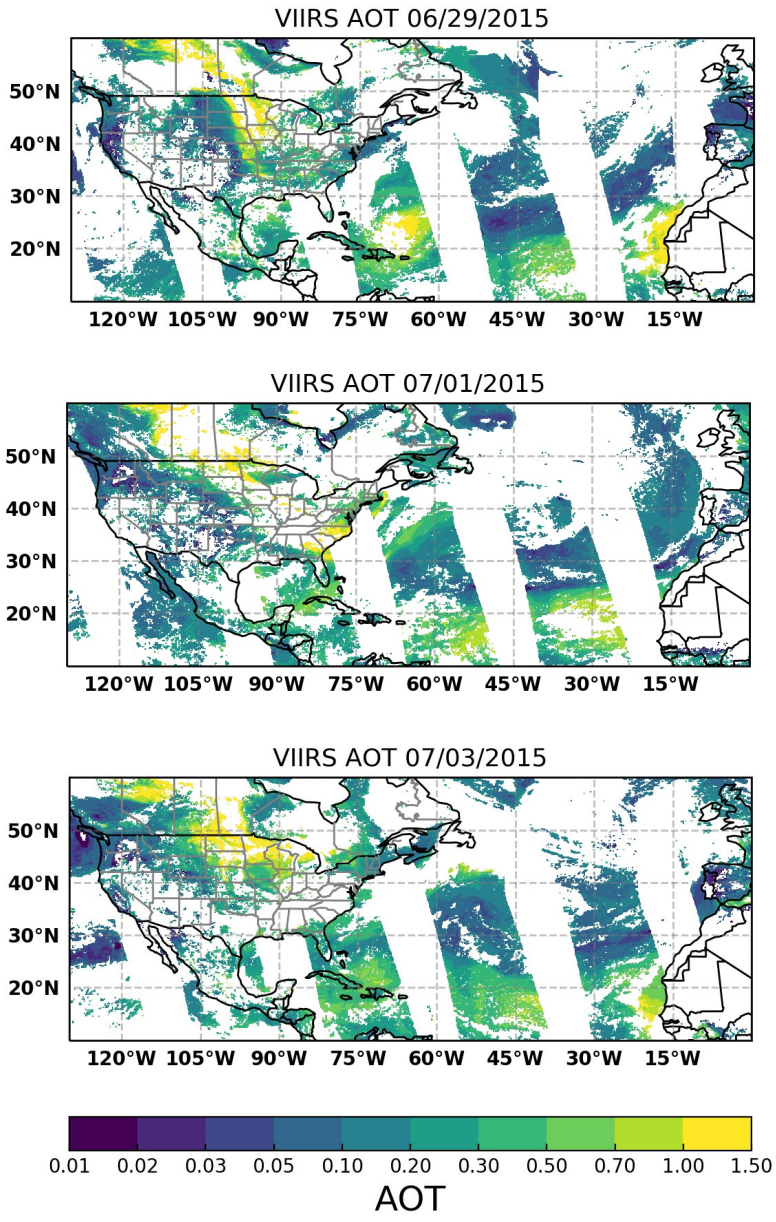

Figure 2. S-NPP VIIRS Aerosol Optical Thickness (AOT) on 06/29, 07/01, and 07/03 of 2015.

Deleted: Figure

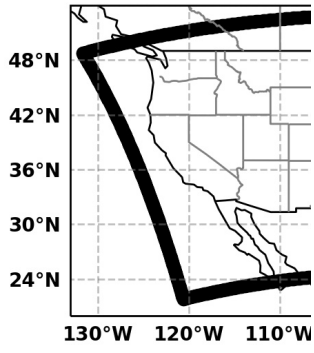

Moved up [1]:
Figure 2, NAQFC CONUS domain (bold black)

Deleted: ¶

Page Break

Formatted: Centered

Deleted: 1

Deleted: ¶

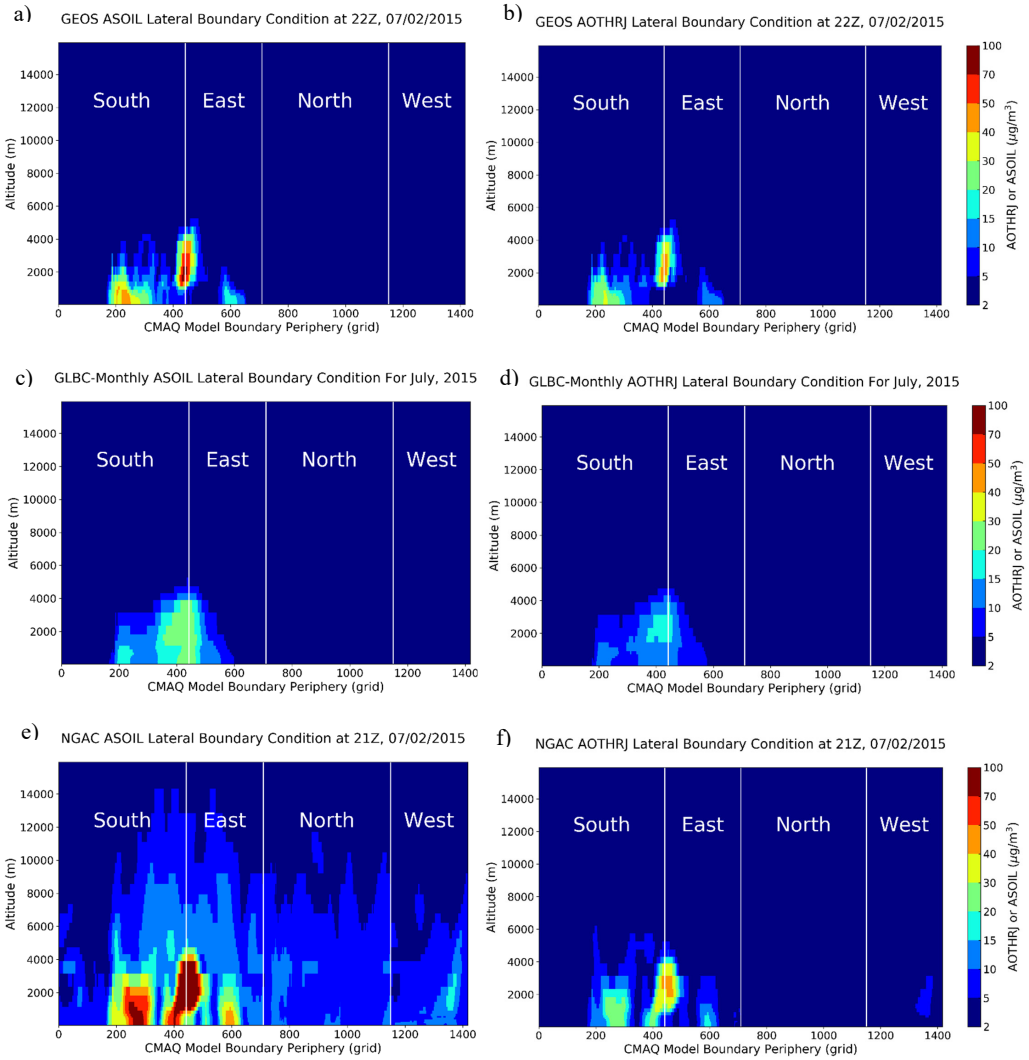

Figure 3. The lateral boundary conditions for ASOIL (left) and AOTHRJ (right) along the domain periphery for July 02, 2015. The CMAQ LBC's grid index for each LBC segment is always from south to north and from west to east, so the LBC index's start-points are reset instead of continuous for the north and west boundaries.

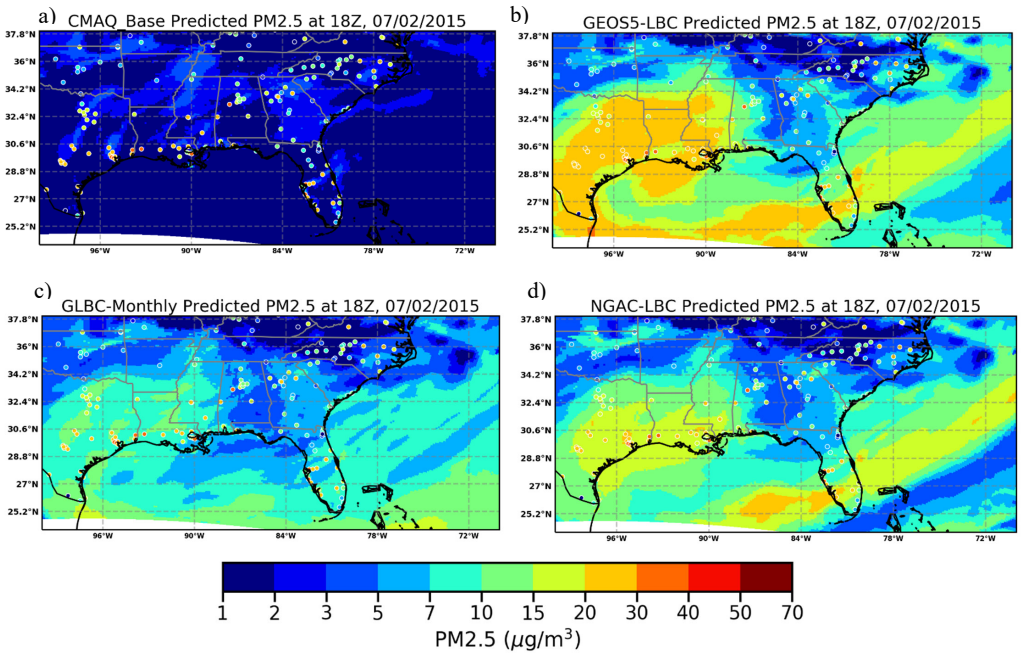

Figure 4. Model Predicted surface PM2.5 with the four LBCs for July 02, 2015 (the colored circles show the AIRNow observations)

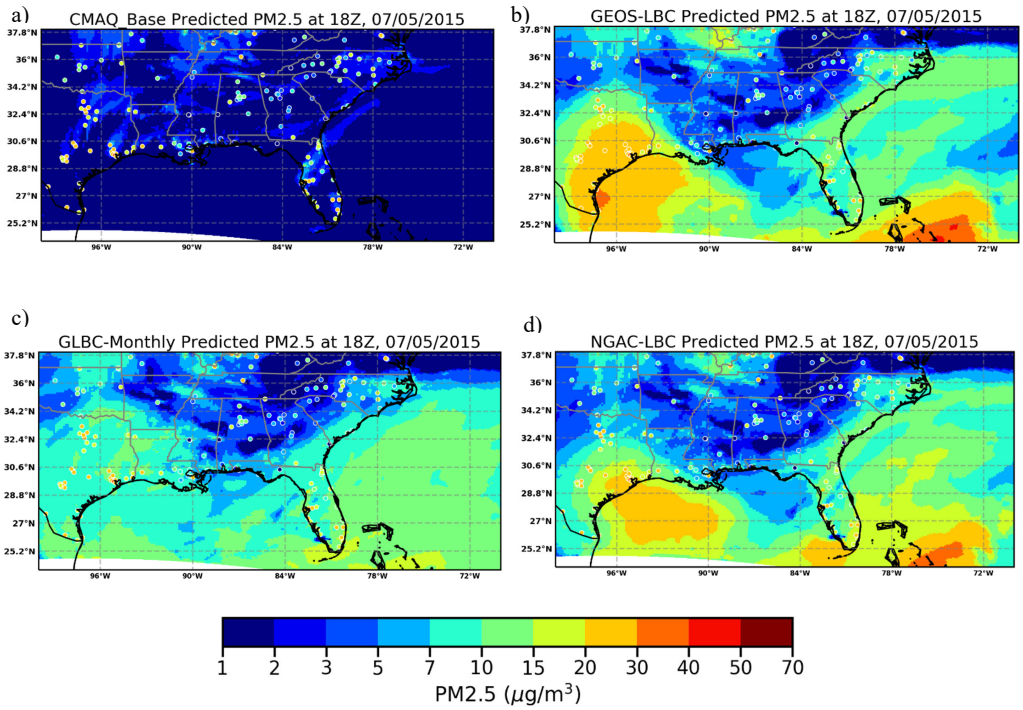

Figure 5. Same as figure 4 but for July 05, 2015

a)

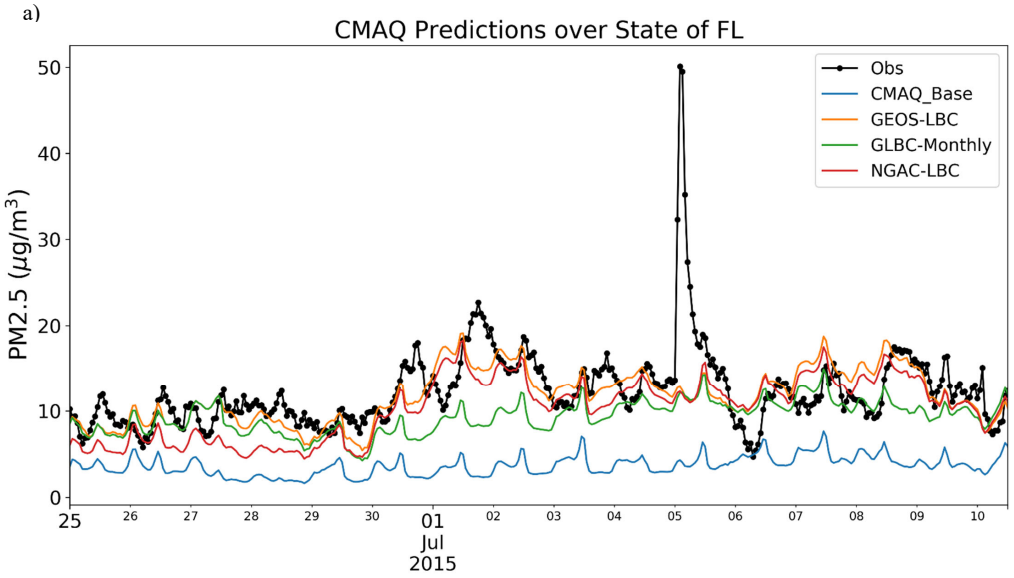

b)

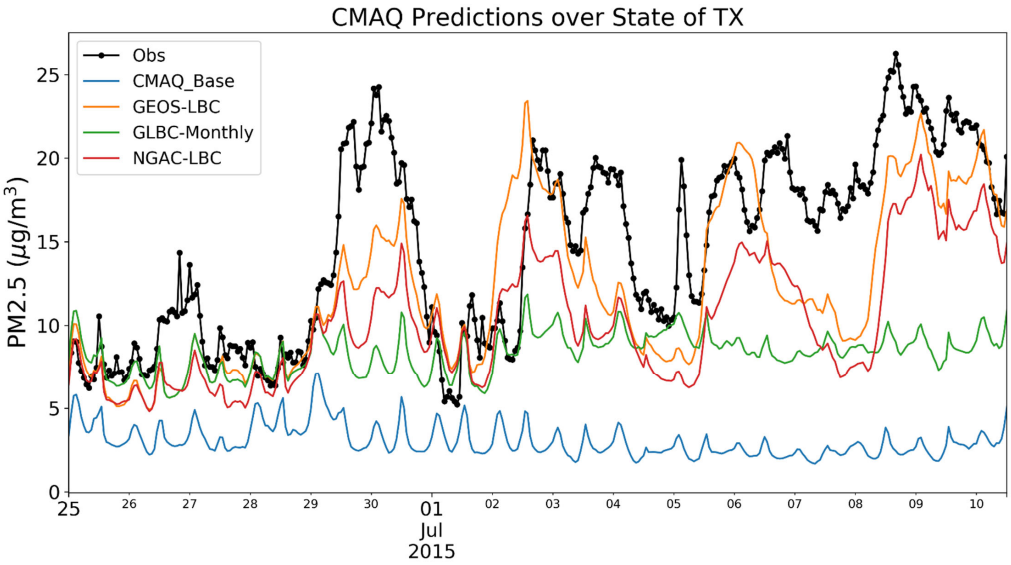

Figure 6. Time-series PM2.5 comparisons over the states of Florida and Texas. All the times are in UTC.

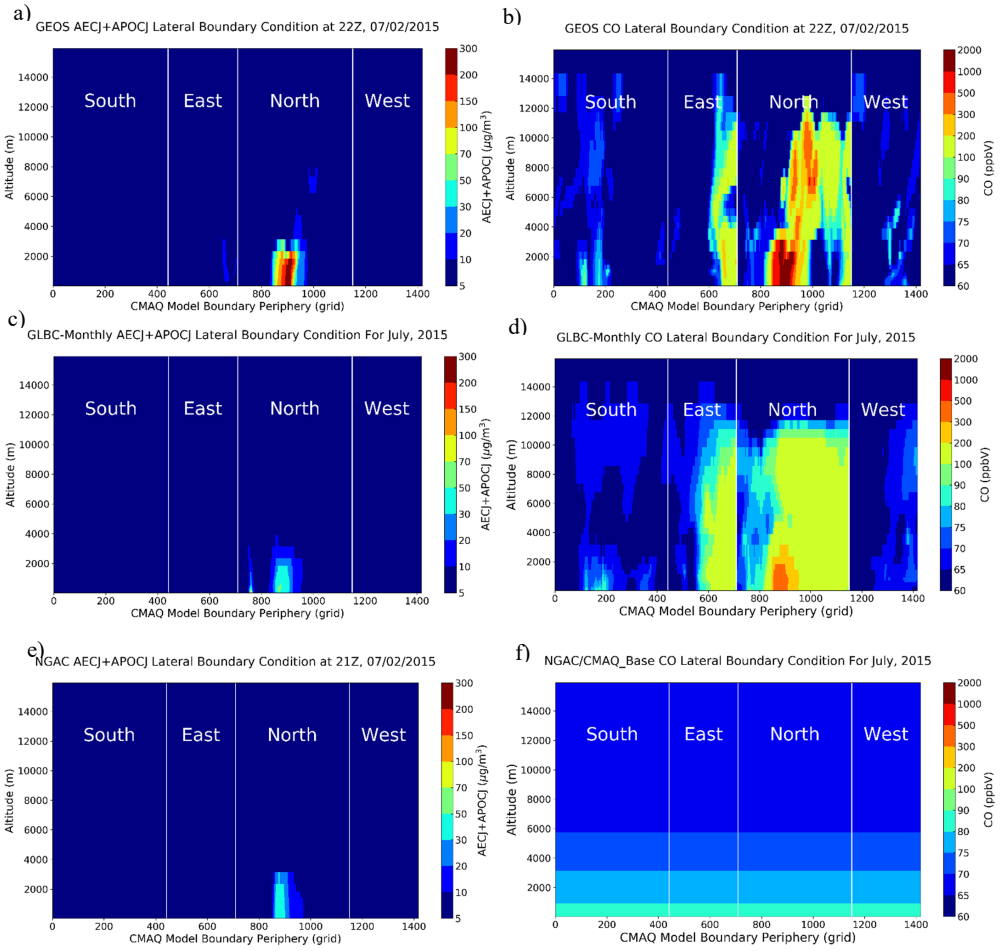

Figure 7, same as Figure 3 except for total EC and POC (AECJ+APOCJ) (left) and CO (right).

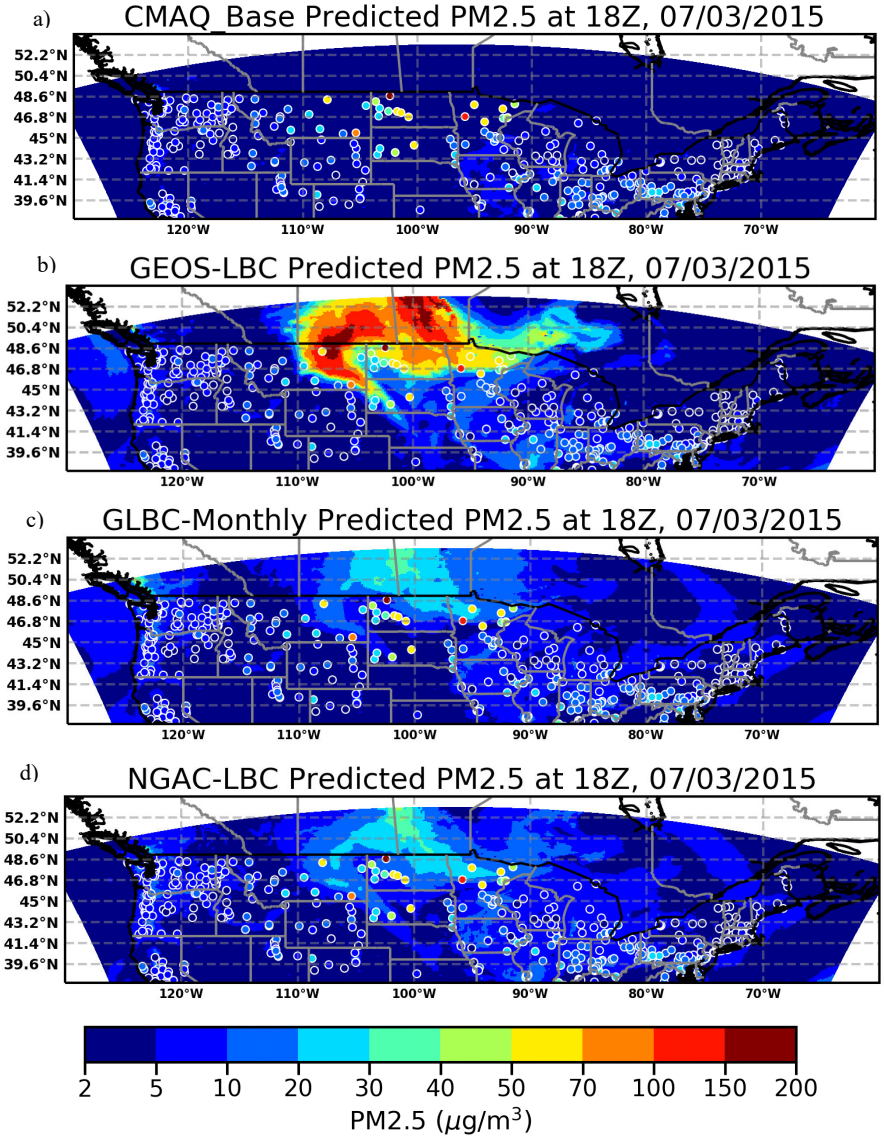

Figure 8, same as Figure 4, but for Northern USA on July 3, 2015

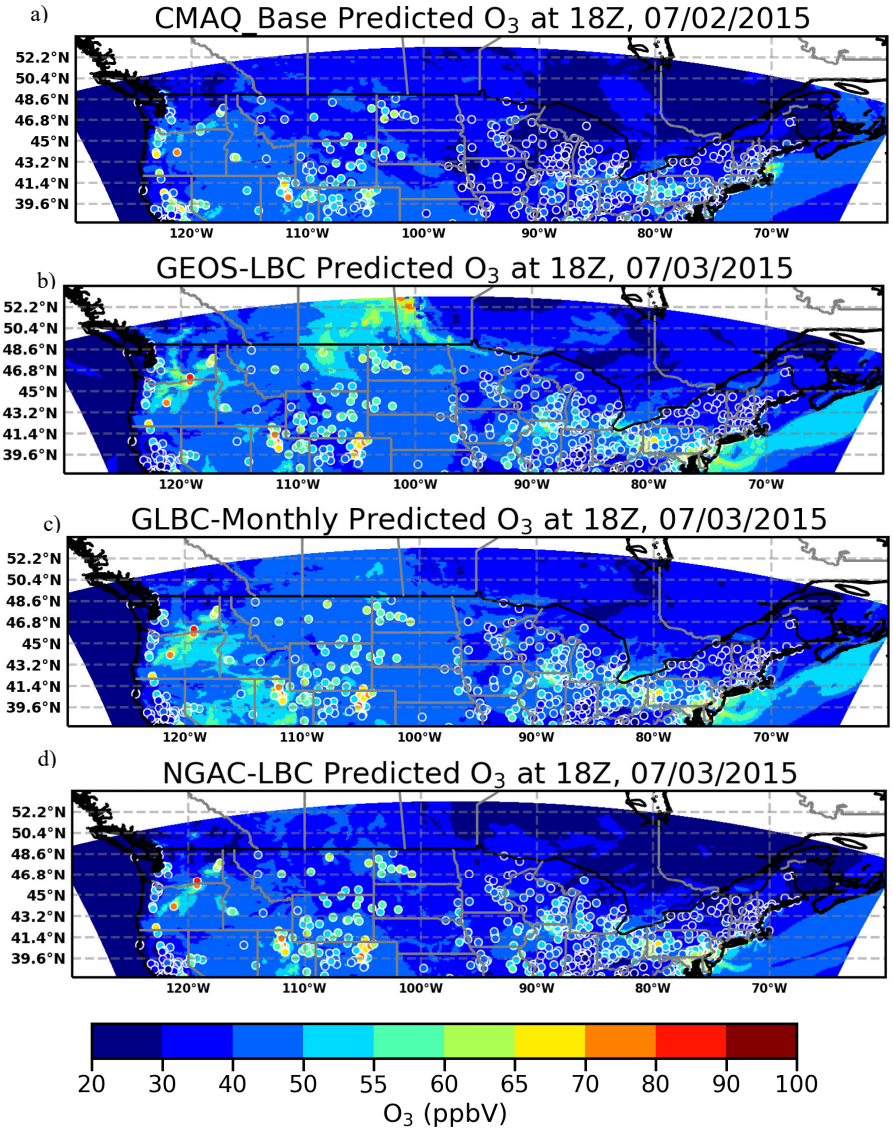

Figure 9, same as Figure 8, but for O_3.

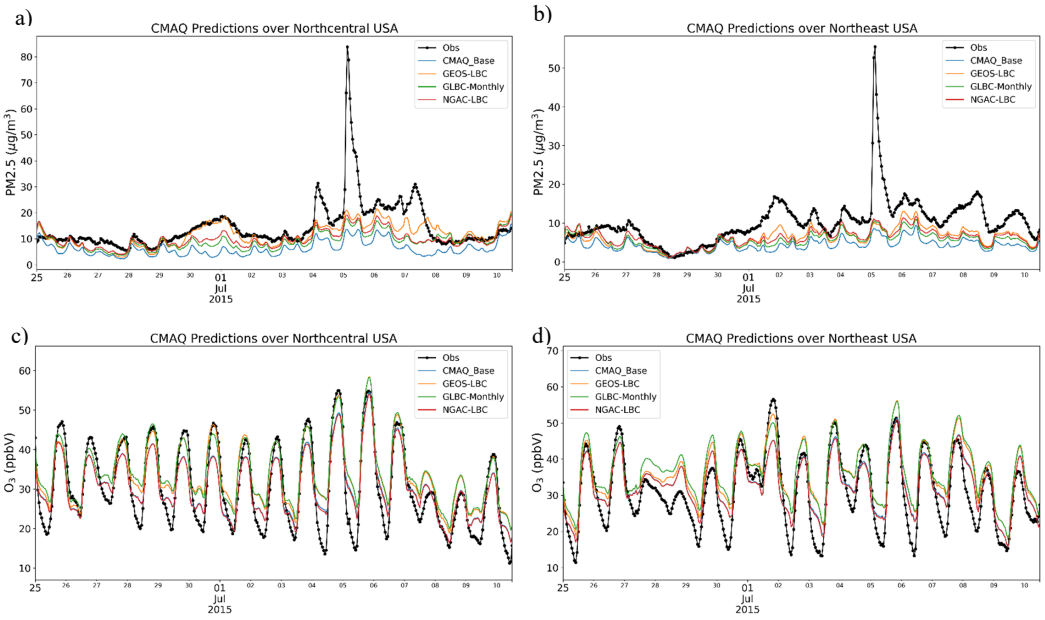

Figure 10. Time-series comparisons for PM2.5 (top) and O_3 (bottom) over the Northcentral (left) (States of Illinois, Indiana, Iowa, Kentucky, Michigan, Minnesota, Missouri, Ohio, and Wisconsin) and Northeastern USA (right) (States of Connecticut, Delaware, Maine, Maryland, Massachusetts, New Hampshire, New Jersey, New York, Pennsylvania, Rode Island and Vermont and District of Columbia). All the times are in UTC.

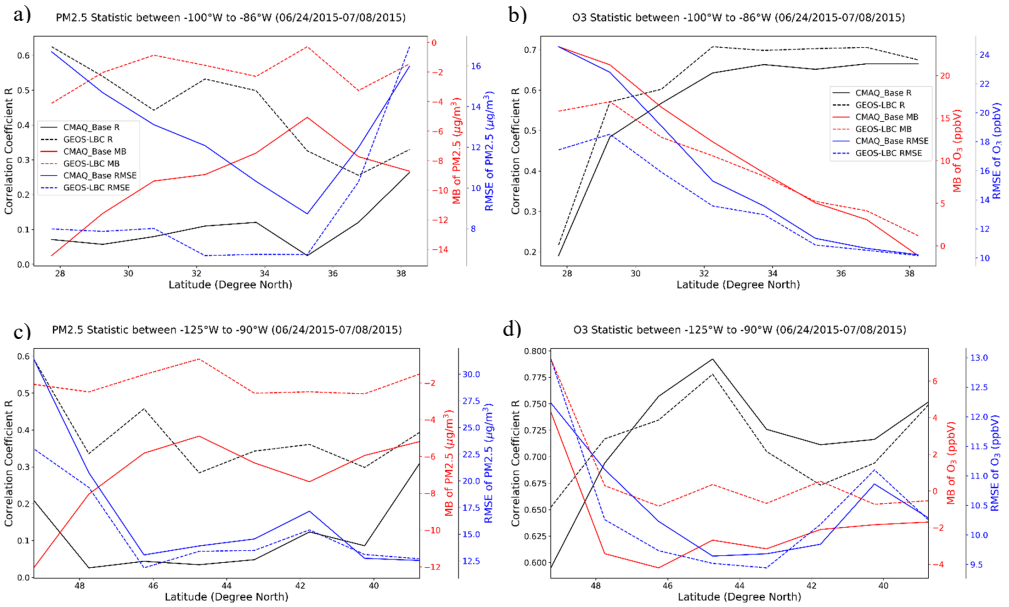

Figure 11, The latitudinal distributions of correlation coefficient R (black), mean bias (MB) (red), and root mean square error (RMSE) (blue) of $PM_{2.5}$ (left) and O_3 (right) from June 24 to July 8, 2015 over Southern USA (top) and Northern USA (bottom) for CMAQ_Base (solid line) and GEOS-LBC (dash line) runs.

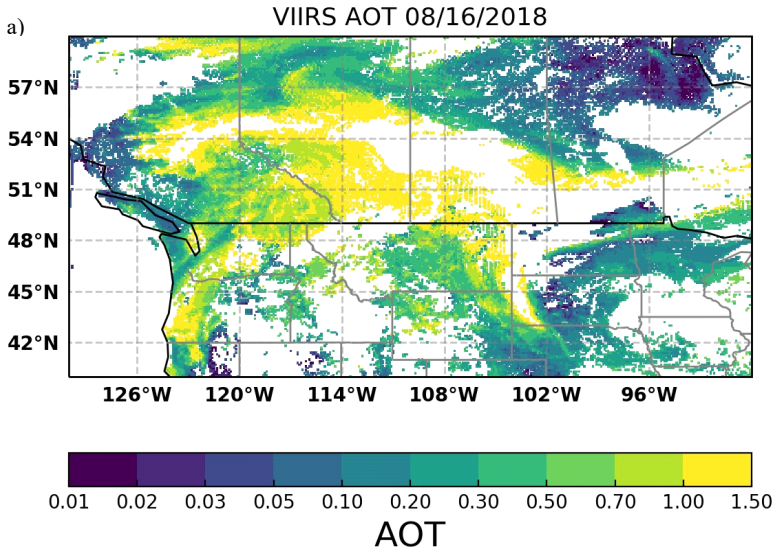

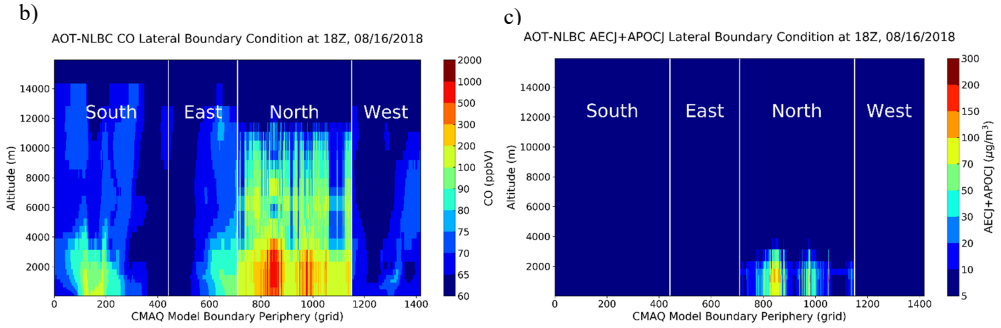

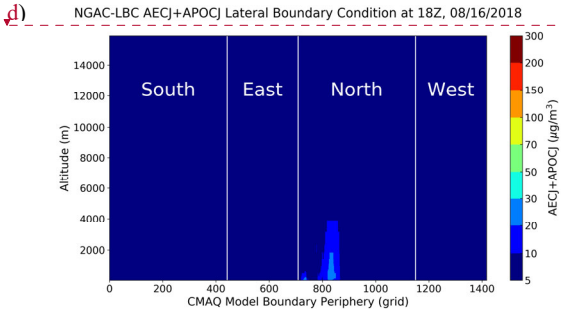

Deleted: a

Formatted: Left

Figure 12. VIIRS-AOT (a) on 08/16/2018 and the corresponding derived AOT-NLBC for CO (b) and AECJ+APOCJ (c). The plot d shows the NGAC-LBC's AEC+APOCJ at the same time.

Deleted: ¶

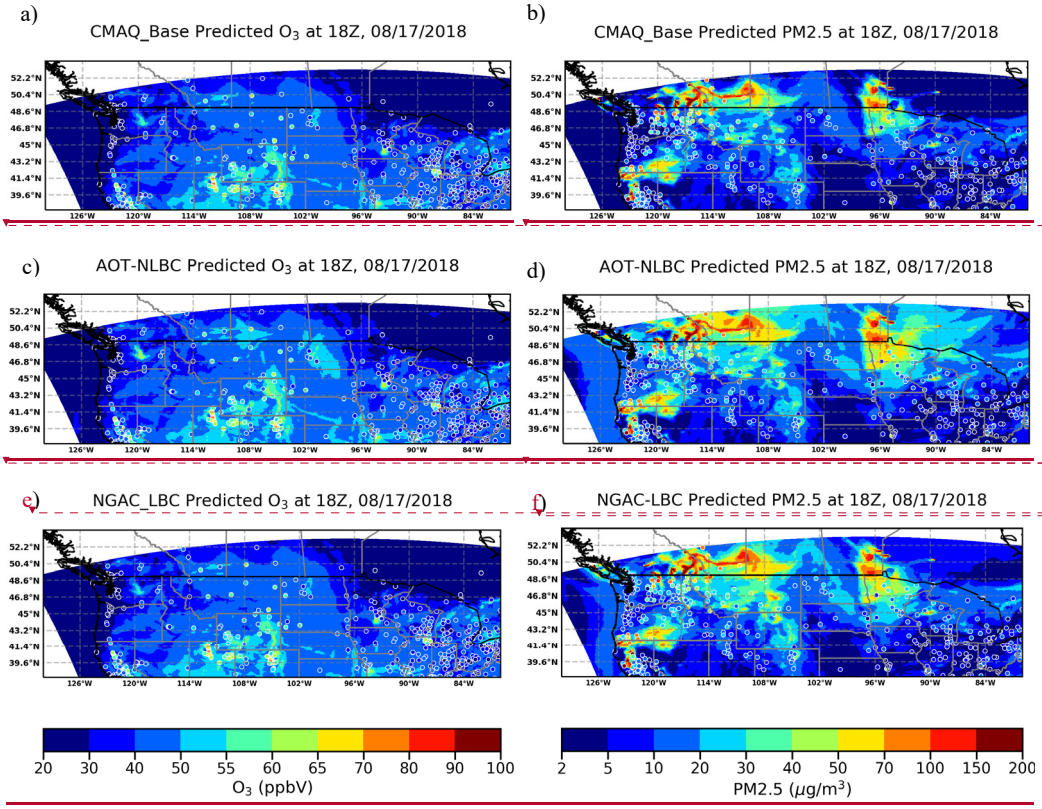

Figure 13. Model Predicted surface ozone (left) and PM2.5 (right) with the CMAQ_Base (a, b), AOT-NLBC (c, d) and NGAC-LBC (e, f) for August 17, 2018 (the colored circles show the AIRNow observations)

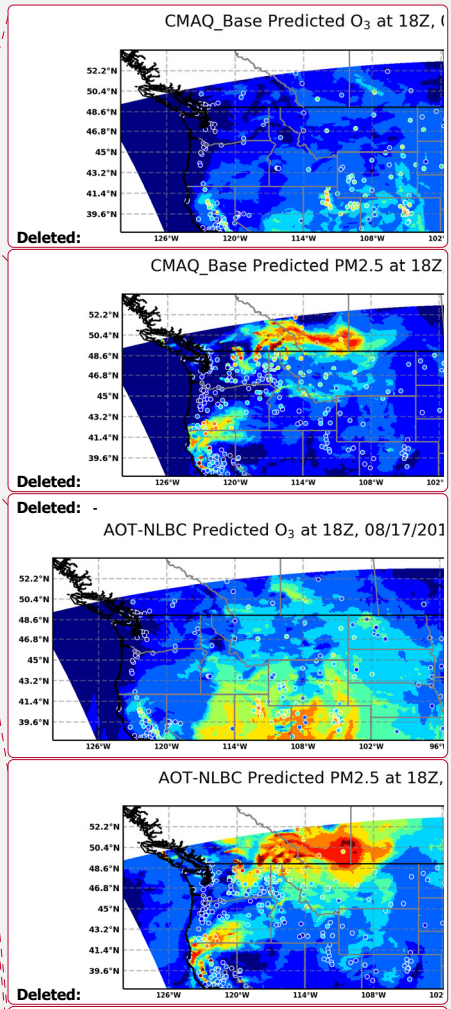

Deleted:

Deleted: -

Deleted:

Deleted: a

Deleted: a

Deleted: top

Deleted: and

Deleted: bottom

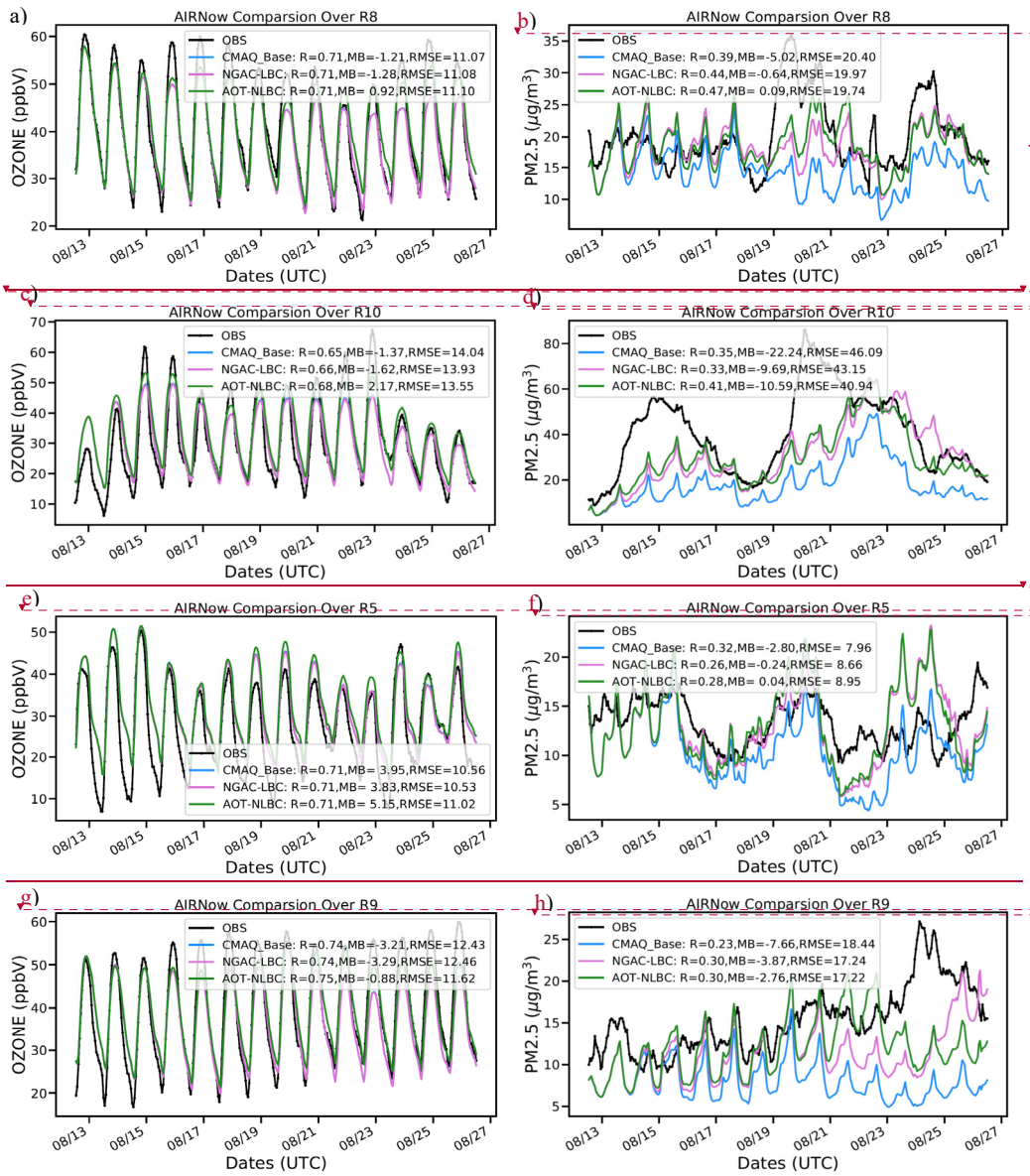

Figure 14, AIRNow time-series comparisons for surface ozone (left) and PM2.5(right) over EPA region 8 (R8, states of MT, ND, SD, WY, CO and UT), region 10 (R10, states of WA, ID and OR), region 5 (R5, states of MN, WI, IL, IN, MI, OH) and region 9 (R9, states of CA, NV, AZ) predicted by CMAQ_Base, NGAC-LBC and AOT-NLBC in 2018

Deleted: ¶

Formatted: Space After: 0 pt

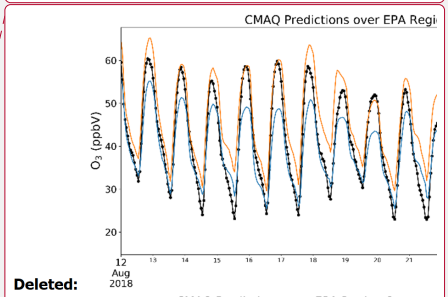

Deleted:

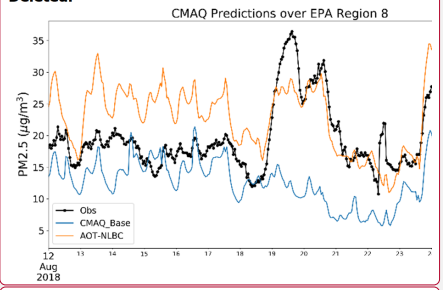

Deleted: a

Deleted: a

Deleted: a

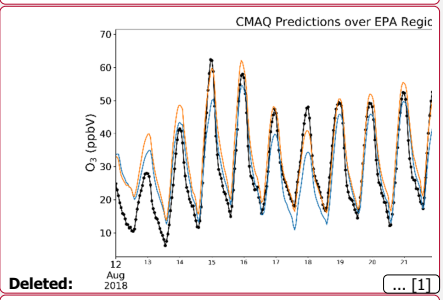

Deleted: ... [1]

Deleted: a

Deleted: a

Deleted: a

Deleted: a

Deleted: Time

Deleted: and